Structural variations across the nepheline ($NaAlSiO_4$)-kalsilite ($KAlSiO_4$) series

Running head: Nepheline-kalsilite series

SYTLE M. ANTAO[1,*] AND GUY L. HOVIS[2]

[1]Department of Geoscience, University of Calgary, Calgary, Alberta T2N 1N4, Canada

[2]Department of Geology & Environmental Geosciences, Lafayette College, Easton, PA 18042, USA

ABSTRACT

The crystal structure of 19 samples from the nepheline ($NaAlSiO_4$; Ne) -kalsilite ($KAlSiO_4$; Ks) series, previously prepared via ion-exchange, were examined using synchrotron high-resolution powder X-ray diffraction (HRPXRD) data and Rietveld structure refinements. Parent materials for the three series include a natural Monte Somma nepheline (series-1), synthetic Na nepheline (series-2), and high-Si synthetic nepheline (series-3) having excess Si mole percentages of 5.2%, 1.7%, and 12.5%, respectively. Three different structure-types were found to occur among the samples examined: nepheline ($P6_3$), tetrakalsilite ($P6_3$), and kalsilite (both $P6_3$ and $P31c$ intergrowth). Trikalsilite was not observed in this study. Vacancies (□) at the K site as well as Ca and K atoms at the Na1 site play an important role in the crystal chemical behaviour of nepheline solid solutions. Vacancies cause an elongation in the average <K-O>[9] distance in nepheline. When K atoms enter the Na1 site in nepheline, the average <(Na,K) -O>[7] distance increases linearly and is parallel to the average <(Na,K)-O>[9] distance in kalsilite and the grand mean of such distances in trikalsilite and tetrakalsilite. Before K atoms enter the Na1 site, the average <(Na,K)-O>[7] distance is constant because of the full occupancy of the Na1 site with Na atoms. Ca atoms at the Na1 site in the Monte Somma sample-1 cause a contraction in the <(Na,K)-O>[7] distance. In Na-rich nepheline samples, Na atoms in the large channels occupy a Na(K) site that is off the 6_3 axis and close to the usual K site. In natural nepheline samples, the K site in most cases contains K atoms and □, and the Na1 site is filled mainly with Na, minor Ca, and K atoms in K-rich samples. Nepheline from Monte Somma (sample-1) contains weak satellite reflections that are also present in some other kalsilite samples. Average <*T*-O> distances indicate a high degree of Al-Si disorder in nepheline, but increasing Al-Si order in tetrakalsilite and kalsilite. Increasing the amount of K atoms beyond the ideal composition of $K_{0.25}Na_{0.75}[AlSiO_4]$ causes expansion in multiple structural parameters because of the larger size of K^+ relative to Na^+.

Keywords: Nepheline-kalsilite series, crystal structure, Al-Si order, HRPXRD, satellite reflections.

*E-mail: antao@ucalgary.ca

INTRODUCTION

Nepheline (ideally $Na[AlSiO_4]$; Ne) and kalsilite (ideally $K[AlSiO_4]$; Ks) are framework minerals in which corner-linked SiO_4 and AlO_4 tetrahedra form so-called "stuffed tridymite" framework structures with half the Si replaced by Al atoms, and with Na, Ca, and K as extra framework charge-balancing cations (e.g., Schiebold 1930; Buerger et al. 1954; Hahn and Buerger 1955; Sahama 1958; Capobianco and Carpenter 1989; McConnell 1991; Carpenter and Cellai 1996; Xu and Veblen 1996). The extra framework cations occur in channels confined by rings of tetrahedra having different shapes and diameters (Figs. 1, 2). IMA recommends $Na_3K(Al_4Si_4O_{16})$ with Z = 2 as the ideal formula for nepheline (Hålenius et al. 2018). However, in this paper we are using the simplified formulae above to represent the Ne-Ks series.

Nepheline commonly contains an excess of Si over Al atoms, which creates vacancies (□) because of $□Si^{4+} = (K,Na)^+Al^{3+}$ and $□Ca^{2+} = 2(K,Na)^+$ substitutions; this is reflected by the generalized formula $(K,Na,□)_{1-x}[Al_{1-x}Si_{1+x}O_4]$ where x represents the "excess" of Si over Al atoms. In end member $Na[AlSiO_4]$, Na atoms are not expected to be at the K site because of the smaller size of Na.

Between nepheline $Na[AlSiO_4]$ and kalsilite $K[AlSiO_4]$ end-members, trikalsilite and tetrakalsilite structures occur over specific compositional ranges, though trikalsilite was not found in the present study. The structures of nepheline, trikalsilite, tetrakalsilite, and kalsilite are not isostructural. Although these four different hexagonal structures have nearly the same $c \approx 8.5$ Å unit-cell parameter, they differ in their a unit-cell parameter: $a_{Ks} \approx 5$ Å in kalsilite, $a \approx 10$ Å (= 2 x a_{Ks}) in nepheline, $a \approx 15$ Å (= 3 x a_{Ks}) in trikalsilite, and $a \approx 20$ Å (= 4 x a_{Ks}) in tetrakalsilite. Note that natural tetrakalsilite is called panunzite, which occurs at Somma-Vesuvius area, Italy (Benedetti et al. 1977), whereas natural trikalsilite occurs near Mt. Nyiragongo, Virunga volcanic field, North Kivu, Zaire (Bonaccorsi et al. 1988).

Most natural nepheline samples have a composition close to $K_2Na_6[Al_8Si_8O_{32}]$ with a K site that contains K atoms and vacancies. However, nepheline specimens from a few rare K-rich volcanic rocks display structures in which K atoms and vacancies occupy the K site and the remaining K atoms replace some of the Na atoms at the Na1 site. Such volcanic

nepheline samples have unusual chemical compositions and large unit-cell parameters that extend the natural nepheline solid solutions considerably (Antao and Nicholls 2018; Hamada et al. 2018). Because nepheline has a Na/K ratio of 3:1, the ideal formula corresponds to $(NaAlSiO_4)_{0.75}(KAlSiO_4)_{0.25}$ or $Ne_{0.75}Ks_{0.25}$ with the formula $K_{0.25}Na_{0.75}[AlSiO_4]$. Ideally, with Ks > 0.25, additional K atoms enter the Na1 site. Without K, as in $Na_8[Al_8Si_8O_{32}]$, Na atoms in the 6_3 channels occur at a Na(K) site that is close to the usual K site (Fig. 1).

In the present study, nineteen Ne-Ks samples across a wide compositional spectrum were examined using synchrotron high-resolution powder X-ray diffraction (HRPXRD) data and Rietveld structure refinements. Our primary aims were to obtain the crystal structures of nepheline samples that are far more Na-rich than previously-studied natural specimens, explore the structures of nepheline - tetrakalsilite - kalsilite minerals at a greater number of compositions than have been studied previously, determine Ne-Ks structural changes as a function of Al:Si ratio, understand the systematics of structural change as a function of Na:K ratio across the Ne-Ks system, and provide valuable structural characterization to Ne-Ks specimens studied thermodynamically via solution calorimetry (Hovis et al. 1992; Hovis and Roux 1993). The latter publications on these synthetic samples provided unit-cell parameters.

STRUCTURAL BACKGROUND INFORMATION

Nepheline

The structures of nepheline specimens from various geological settings have been refined in space group $P6_3$ by numerous investigators (Dollase 1970; Foreman and Peacor 1970; Dollase and Peacor 1971; Simmons and Peacor 1972; Dollase and Thomas 1978; Gregorkiewitz 1984; Hassan et al. 2003; Tait et al. 2003; Gatta and Angel 2007; Angel et al. 2008; Antao and Hassan 2010). Crystal structures in the nepheline - kalsilite series have been discussed by Merlino (1984) and Palmer (1994). The nepheline structure consists of four independent tetrahedral Al and Si sites per unit cell (Fig. 1a). The Si1 and Al1 sites occupy special positions on three-fold axes, whereas the Si2 and Al2 sites occupy general positions. The apices of Si tetrahedra point in one direction along the **c** axis, whereas the Al tetrahedra point in the opposite direction. In both nepheline and kalsilite, the apical oxygen atom, O1, is

slightly off the threefold axis (Figs. 1a, 2a). Na atoms occupy six small oval-shaped cavities (6*c* Na1 site), and K atoms occupy two large hexagonal-shaped channels (2*a* K site), which gives $Na_6K_2[Al_8Si_8O_{32}]$ as the ideal nepheline formula. In natural samples, small amounts of Ca also may occur with Na and K atoms at the Na1 site, with vacancies and K atoms at the K site. In Na-rich nepheline samples, some Na atoms occupy a Na(K) site, which is located close to but physically distinct from the K site (Fig. 1). Indeed, such a Na(K) site has been found in other studies (Dollase and Thomas 1978; Hippler and Böhm 1989; Rossi et al. 1989).

Diffraction data from some nepheline samples show satellite reflections with a wide range of intensity and sharpness (Sahama 1958; McConnell 1962; Sahama 1962; McConnell 1981, 1991; Hassan et al. 2003; Antao and Hassan 2010). The satellite reflections indicate that nepheline has a modulated structure with an incommensurate supercell. Various models have been proposed for the modulated structure of nepheline (McConnell 1962; Parker and McConnell 1971; Parker 1972; McConnell 1981, 1991; Hayward et al. 2000; Angel et al. 2008). Recently, a model for the incommensurately modulated structure of nepheline was presented in a superspace group by Friese et al. (2011) indicating that all the atoms in the structure are displacively modulated with amplitudes below 0.1 Å.

Kalsilite

The kalsilite structure has been refined in a number of space groups, including $P6_3$ (Perrotta and Smith 1965; Kremenović and Vulić 2014), $P31c$ (Cellai et al. 1997; Gatta et al. 2010), and $P6_3mc$ (Dollase and Freeborn 1977; Andou and Kawahara 1982). In addition, an abstract reported a kalsilite structure in space group $P6_322$ (Uchida et al. 2006). Kalsilite having monoclinic symmetry has been reported by Kremenović et al. (2013). The kalsilite structure was studied at high temperature (Kawahara et al. 1987) and high pressure (Gatta et al. 2011). The framework structure of kalsilite contains layers of alternating AlO_4 and SiO_4 tetrahedra where AlO_4 tetrahedra point downwards and SiO_4 tetrahedra point upwards (Fig. 2a). The sheets of ordered Al-Si atoms are stacked along [001] and joined through the apical O1 atoms. The O1 site is disordered over three nearby positions that are similar to the O1 site in

nepheline. Moving the O1 site off the 3-fold axis by 0.25 Å causes a reduction of the Al-O1-Si angle from the unfavorable value of 180 to about 160°. The K sites occur in ditrigonal rings. The 9-fold coordination of K gives an average <K-O>[9] of 3.0 Å, which is similar to that in nepheline. All six-membered rings in kalsilite are ditrigonally distorted and stacked along the **c** axis, connected through the apical O1 atoms in a staggered conformation such that all ditrigonal rings in one layer "point" in one direction and all ditrigonal rings in the next layer "point" in the opposite direction. Individual layers of *P*31*c* kalsilite structure are essentially the same as those of the $P6_3$ kalsilite structure, but the layers are stacked in an eclipsed manner such that ditrigonal rings in both adjacent layers "point" in the same direction.

Tetrakalsilite and trikalsilite

The structure of tetrakalsilite (natural panunzite) was refined by Merlino et al. (1985). The framework structure of tetrakalsilite contains layers of alternating AlO_4 and SiO_4 tetrahedra with AlO_4 tetrahedra pointing upwards and SiO_4 tetrahedra pointing downwards (Fig. 3). The K1 and K3 sites are in ditrigonal rings, K5 sites are in hexagonal rings, and K2, K4, and Na1 sites occupy oval-shaped rings. Of the six alkali sites, Na1 contains 100% Na, K3 and K5 contain 100% K. The remaining sites contain different amounts of Na atoms, K1, K2, and K4 having 12, 22, and 17% Na, respectively (Merlino et al. 1985).

Refinement of the trikalsilite structure reveals a hexagonal $P6_3$ ordered Al-Si framework structure containing hexagonal, ditrigonal, and oval-shaped rings (Bonaccorsi et al. 1988). The M1, M4, and M5 sites contain only K atoms, whereas M2 contains 0.7 Na and 0.3 K and M3 contains 0.3 Na and 0.7 K. The grand mean distance of the alkali sites is 2.931 Å.

The framework structure of minerals in the Ne-Ks series contains six-membered rings having different shapes. Nepheline has hexagonal and oval rings, kalsilite hexagonal and ditrigonal rings, and tetrakalsilite hexagonal, oval, and ditrigonal rings. In successive layers, the tetrahedra are in an eclipsed relation in trikalsilite and tetrakalsilite, but in a staggered relation in nepheline and kalsilite.

This is the peer-reviewed, final accepted version for American Mineralogist, published by the Mineralogical Society of America.
The published version is subject to change. Cite as Authors (Year) Title. American Mineralogist, in press.
DOI: https://doi.org/10.2138/am-2021-7484. http://www.minsocam.org/

SAMPLE DESCRIPTION

This study examines the crystal structures of 19 samples from nepheline (Ne; $NaAlSiO_4$) to kalsilite (Ks; $KAlSiO_4$) that were made by ion exchange from sodic parent materials (e.g., Hovis et al. 1992; Hovis and Roux 1999; Hovis et al. 2009). The so-called "natural" series (referred to as series-1 in this study) was made by K-Na ion exchange of a natural nepheline sample-1 (= 8311) from Monte Somma, Italy, with composition $(Na_{0.747}Ca_{0.036}K_{0.129}\square_{0.088})[Al_{0.948}Si_{1.052}O_4]$ containing 5.2 mole % excess Si atoms, 3.6 mole % Ca atoms, and vacancies totaling 8.8 %, $\square_{0.088} = Si_{0.052} + Ca_{0.036}$ (Hovis et al. 1992). The "synthetic" series (referred to as series-2 in this study) was made by K-Na ion exchange of synthetic sodic nepheline sample-6 (= 880408), $(Na,K)_{0.983}\square_{0.017}[Al_{0.983}Si_{1.017}O_4]$, hydrothermally synthesized from a gel containing 1.7 mole % excess Si atoms and the same amount of vacancies (Hovis et al. 1992; Hovis and Roux 1993). A "high-Si" series (designated as series-3 in this study) made from sodic end member sample-16 (= 9504) contains 12.5 mole % excess Si atoms (Hovis and Roux 1999; Hovis and Crelling 2000; Hovis et al. 2009). Four chemical components were used to describe compositions in the nepheline–kalsilite series, including Ne ($NaAlSiO_4$), Ks ($KAlSiO_4$), 2Qz ($\square Si_2O_4$), and 0.5An ($\square_{0.5}Ca_{0.5}AlSiO_4$), where X_{Ne} and X_{Ks} indicate the mole fraction (X) of Ne and Ks, respectively, $\square$ are vacancies (Vac), and $X_{Vac} = X_{2Qz} + 0.5\ X_{0.5An}$. Mole fractions of sodium, potassium, calcium, and vacancies are related to chemical components as: $X_{Na} = X_{Ne}$, $X_K = X_{Ks}$, $X_{Ca} = 0.5\ X_{0.5An}$, and $X_{Vac} = X_{2Qz} + 0.5\ X_{0.5An}$. Further details are given in the references above where unit-cell parameters are plotted against compositions for each Ne-Ks series. Note that tetrakalsilite has the ideal formula $K_{0.625}Na_{0.375}[AlSiO_4]$. Table 1 contains the compositions of samples used in this study.

EXPERIMENTAL

Crystals of the Monte Somma sample-1 were hand-picked under a binocular microscope. All the samples were crushed to a fine powder in an agate mortar and pestle for synchrotron high-resolution powder X-ray diffraction (HRPXRD) experiments performed at

beamline 11-BM, Advanced Photon Source, Argonne National Laboratory. The crushed samples were loaded into Kapton capillaries (0.8 mm internal diameter) and rotated during the experiment at 90 rotations per second. The data were collected at 298 K to a maximum 2θ of about 50° with a step size of 0.001° and a step time of 0.1s per step. The HRPXRD traces utilized a unique multi-analyzer detection assembly consisting of twelve independent silicon (111) crystal analyzers and $LaCl_3$ scintillation detectors that reduce the angular range to be scanned and allow rapid acquisition of data. A silicon (NIST 640c) and alumina (NIST 676a) standard (ratio of ⅓ Si : ⅔ Al_2O_3 by weight) was used to calibrate the instrument and refine the monochromatic wavelength used in the experiment ($\lambda \approx 0.4128$ Å; see Table 2). This short wavelength allows rapid accumulation of data over a small 2θ range. Additional details of the experimental set-up are given elsewhere (Antao et al. 2008; Lee et al. 2008; Wang et al. 2008).

RIETVELD STRUCTURE REFINEMENTS

Crystal structures of the samples were modeled by the Rietveld method (Rietveld 1969) using the *GSAS* program (Larson and Von Dreele 2000) and the *EXPGUI* interface (Toby 2001). Initial structural parameters for nepheline were taken from Hassan et al. (2003), for tetrakalsilite from Merlino et al. (1985), for $P6_3$ kalsilite from Perrotta and Smith (1965), and for *P*31*c* kalsilite from Cellai et al. (1997). Scattering curves for neutral atoms were used. The background was modeled with a Chebyschev polynomial (8 terms). In the *GSAS* program, the reflection-peak profiles were fitted using type-3 profile (pseudo-Voigt; Cagliotti et al. 1958; Thompson et al. 1987). Structure refinements were carried out by varying parameters in the sequence: scale factor, background, unit-cell parameters, zero shift, profile, atom positions, isotropic displacement parameters, and site-occupancy factor (*sof*) (Table 1). Finally, all variables were refined simultaneously. The isotropic displacement parameters for all the Al and Si sites were constrained to be equal and those for all the O sites were constrained to be equal to each other. Except for sample-1, the "extra" reflections present in some samples were not deleted, which resulted in higher χ^2, but the R_F^2 value is unaffected; the latter is a better guide for the quality of a good structure refinement. The nepheline

samples are well refined (R_F^2 < 7%) and the other samples have R_F^2 less than 10% (Table 2). The number of observed reflections for each sample is given in Table 2 together with the total number of variables. In the two-phase refinement of kalsilte, all the variables were refined simultaneously because the ratio of the observed reflections to variables is quite high (≈ 20; see Table 2b). There were no correlation problems. In addition, the resulting structures for both of the kalsilite phases are similar to those given in the literature. Nepheline contains a disordered O1 site, so a soft T-O1 distance constraint was used to refine the O1 site to obtain reasonable T-O1 distances (Table 4a). In the other samples, T-O distance constraint was used (Tables 4b, 4c)

The compositions obtained by the Rietveld refinements agree well with those of the chemical analyses (Table 1). The unit-cell parameters and other information regarding data collection and refinement are given in Table 2a for nepheline and tetrakalsilite, and Table 2b for kalsilite. The positional coordinates and isotropic displacement parameters for 11 nepheline samples are given in Table 3a, for one tetrakalsilite sample in Table 3b, and for six kalsilite samples in Tables 3c and 3d. Bond distances and bridging angles for nepheline, tetrakalsilite, and kalsilite are given in Tables 4a, 4b, and 4c, respectively. Tables 2, 3, and 4 are deposited[1].

RESULTS AND DISCUSSION

HRPXRD traces for samples from the nepheline-kalsilite series contain different characteristic features. The most Na-rich nepheline samples of the three series are shown in Figures 4 and 5. Samples-16 and -6 (original sample numbers of Hovis and coworkers are given in column 2 of Table 1) contain no impurities or satellite reflections, whereas sample-1 from Monte Somma does contain weak satellite reflections (Figs. 4c and 5c). The latter are few, but similar to those observed in samples from the Bancroft area (Antao and Hassan 2010). HRPXRD traces for four samples (2 nephelines, 1 tetrakalsilite and 1 kalsilite) are shown for comparison in Figure 6. Nepheline sample-8 contains no impurity peaks or satellite reflections. Nepheline sample-12 contains two different nepheline phases (12a = 79.6(2) and 12b = 20.4(5) wt. % of the two phases). Tetrakalsilite sample-13 contains what appear to be

weak satellite reflections. Tetrakalsilite sample-2 contains several strong extra peaks (not shown), so the structure was not refined, although unit-cell parameters were indeed obtained (Table 2a). The HRPXRD trace for kalsilite sample-15 is given in Figure 6d. The traces for the three different phases are different from each other.

The $P31c$ to $P6_3$ transition in kalsilite was detected as a change in the intensities of the *hhl* reflections. Those with l = even (e.g., 112) decrease in intensity, whereas those with l = odd (e.g., 111) increase (Cellai et al. 1999). Note that the 112 reflections overlap in both space groups. In our six kalsilite samples, 111 reflections are always present, indicating space group $P6_3$. Figure 7 shows parts of expanded traces for the six kalsilite samples.

In previous studies, the structure of a volcanic kalsilite sample was refined in the space group $P6_3$ by Perrotta and Smith (1965) and that for a metamorphic kalsilite sample in the space group $P31c$ by Cellai et al. (1997). Reflections *hhl*, l = odd are absent in space group $P31c$, but present in space group $P6_3$. Kalsilite made from nepheline by K-exchange (with *hhl*, l = odd reflections with intensities differing from crystal to crystal) was refined by Dollase and Freeborn (1977) in space group $P6_3mc$ using a crystal with *hhl*, l = odd reflections absent. This structure is similar to $P6_3$ kalsilite, but the basal O2 sites are disordered between two mirror equivalent sites, giving rise to an average $P6_3mc$ structure. A similar domain structure was found in synthetic kalsilite prepared by hydrothermal methods (Andou and Kawahara 1984). Na-poor and Na-free kalsilite crystals prepared from nepheline by K-exchange are composed of (001) domains with space groups $P6_3$ and $P31c$ (Xu and Veblen 1996).

In this study, all six kalsilite samples contain two phases with space groups $P6_3$ and $P31c$. From Figure 7a to Figure 7e, the wt. % of the $P6_3$ kalsilite phase decreases from 99.33(1) % to 22.2(1) %. This is also reflected in the intensities of the 111 reflections that decrease from Figure 7a through 7e. All the reflections including the 111 in Figure 7f are broad, compared to those of other samples. As the 111 intensity decreases, the 112 intensity tends to increase indicating increasing amounts of the $P31c$ kalsilite phase (with 112 reflections overlapping in both phases). Weak unfitted satellite reflections are present in Figures 7b, 7e, and 7f; these are easily observed in the difference curves. As in kalsilite,

intergrowths of two or more distinct phases also occur in other minerals (e.g., Antao 2013b, a; Antao and Klincker 2013).

Three nepheline samples (6, 7, 17) contain both K and Na(K) sites that are close enough to each other to be considered a split site (Table 3a). Note that sample-16 contains no K atoms. Vacancies in the 6_3 channels occur at the K and Na(K) sites. The Na1 site is filled with Na atoms in samples-6 and -16. Sample-1 contains only K atoms and some vacancies at the K site. The Na1 site is filled with Na and K atoms in series-2 and -3 samples. There is a slight excess of Si over Al atoms in all samples, but less so in series-2. Overall, the chemical formulae obtained by the Rietveld refinement method (Table 1) agree well with those from previous studies (Hovis et al. 1992; Hovis and Roux 1993).

The unit-cell parameters for nepheline-kalsilite samples (Table 2a, b; Fig. 8) generally agree well with those obtained in previous studies (Hovis et al. 1992; Hovis and Roux 1999; Hovis et al. 2009). Linear trends are observed among unit-cell parameters for nepheline-kalsilite series that meet at tetrakalsilite (circled points). The red trend lines for nepheline samples were calculated using five data points from the K-rich part of synthetic series-2 (red circles with + in the centre). Red trend lines for kalsilite samples were calculated using data points from both synthetic series-2 and natural series-1 (red and black circles with + in the centre). The linear *a vs. V* plot (Fig. 8*a*) shows little departure from "Literature" data points (Dollase 1970; Foreman and Peacor 1970; Dollase and Peacor 1971; Simmons and Peacor 1972; Dollase and Thomas 1978; Gregorkiewitz 1984; Tait et al. 2003; Angel et al. 2008), including studies indicated in the legend (Sahama 1962; Bonaccorsi et al. 1988; Hovis et al. 1992; Hovis and Roux 1999; Hovis et al. 2009; Antao and Hassan 2010; Vulić et al. 2011; Balassone et al. 2014; Antao and Nicholls 2018; Hamada et al. 2018). Greater scatter is observed in the *c vs. V* plot (Fig. 8*b*), whereas the *c*/*a vs. V* plot (Fig. 8*c*) shows the most scatter. The “high-Si” series-3 deviate the most from the trend lines because of smaller *c* and *c/a* values related to increased amounts of smaller Si vs. larger Al atoms. Similar features are observed in the plot of *c vs. a* (Fig. 9). For comparison to nepheline data, note that *a* unit-cell values for kalsilite are doubled and those for tetrakalsilite are halved (Table 2a, b).

Among the various samples, it is Na-rich nepheline samples that have the smallest volumes. Figures *8a-c* show seven data points that are off the nepheline red trend lines, most clearly seen in Figure 8*c*, corresponding to $V < 726$ Å^3 and Ks < 0.23 (sample-9; Table 2a). Tuttle and Smith (1958) indicated that this point occurs where Na:K = 3:1 in the formula $K_{0.25}Na_{0.75}[AlSiO_4]$ (or $Ne_{0.75}Ks_{0.25}$) where the unit-cell structural formula is ideally $K_2Na_6[Al_8Si_8O_{32}]$. It is on the Na-rich side of this composition that the Na1 site of the nepheline structure is normally filled only with Na atoms (± minor amounts of Ca), but no vacancies. Change in the trend line, therefore, corresponds to the entry of K atoms into the Na1 site (Tables 1, 3a).

In the nepheline structure, the K site is usually on the 6_3 axis and filled with K atoms and vacancies. This gives an average <K-O>[9] distance of about 3 Å. In $Na[AlSiO_4]$ nepheline, the K site is vacant and off the 6_3 axis is a Na(K) site for the Na atoms in the channel, as in sample-16 (Table 3a). With Na atoms at the Na(K) site, reasonable average <Na(K)-O> distances are observed (Table 4a). For Ks < 0.23, some samples (6, 7, and 17; Table 3a) reveal the presence of both the K and Na(K) sites, whereas other samples (1, 8, and 9) contain only the K site. At Ks ≥ 0.23, only the K and Na1 sites are present in the nepheline structure.

For three Na-rich nepheline samples, difference Fourier maps were calculated with K and Na(K) sites omitted from the large 6_3 hexagonal channels (Fig. 10). The K site is on the 6_3 axis in samples-1 and -6 (Fig. 10*b*, *c*). The Na(K) site is off the 6_3 axis in samples-6 and -16 (Fig. 10*a*, *b*). Because K and Na(K) sites are close to each other, they may be regarded as a split site such that both positions cannot be occupied simultaneously. In the structure refinement, if the wrong structural model were used, the isotropic displacement parameters for the Na and Na(K) sites would show unusual values. Sample-16 contains no K atoms and the Na(K) site is occupied (Tables 1, 3a). Moving the Na(K) site off the 6_3 axis gives a smaller average <Na(K)-O>[6] distance of 2.799 Å, which is reasonable for a Na-O bond distance (Table 4a; Fig. 11). In fact, the average <Na(K)-O>[4,6] distance ranges from 2.68 to 2.86 Å. Note that an average <Na(K)-O> distance of 2.61 to 2.62 Å was observed by Dollase and Thomas (1978).

This is the peer-reviewed, final accepted version for American Mineralogist, published by the Mineralogical Society of America.
The published version is subject to change. Cite as Authors (Year) Title. American Mineralogist, in press.
DOI: https://doi.org/10.2138/am-2021-7484. http://www.minsocam.org/

Simmons and Peacor (1972) examined the structure of a nepheline sample from Monte Somma with a composition of $[K_{1.28}\square_{0.72}][Na_{5.36}Ca_{0.28}]_{\Sigma 5.64}[Al_{7.92}Si_{8.08}]O_{32}$, a = 10.003(2), c = 8.381(3) Å, V = 726.251 Å^3, average <K-O>[9] = 3.017 Å, average <Na1-O>[7] = 2.630 Å, <T1-O>[4] = 1.697 Å, <T2-O>[4] = 1.651 Å, <T3-O>[4] = 1.628 Å, and <T4-O>[4] = 1.718 Å. In this study, sample-1 from Monte Somma gave similar results: $[K_{1.24}\square_{0.76}][Na_{5.85}Ca_{0.15}]_{\Sigma 6}[Al_8Si_8O_{32}]$, average <K-O>[9] = 3.018 Å, average <Na1-O>[7] = 2.621 Å, <T1-O>[4] = 1.648 Å for the Si1 site, <T2-O>[4] = 1.719 Å for the Al1 site, <T3-O>[4] = 1.673 Å for the Al2 site, and <T4-O>[4] = 1.674 Å for the Si2 site.

Based on average <Al-O> ≈ 1.74 Å and <Si-O> ≈ 1.62 Å for perfect Al-Si order and T-O ≈ 1.68 Å for complete disorder in framework aluminosilicates (Hassan et al. 2004; Antao et al. 2008), the degree of Al-Si order is variable in Ne-Ks samples (Tables 4a, b, c). Al-Si order is low in nepheline samples (Table 4a), but greater in both tetrakalsilite (Table 4b) and kalsilite (Table 4c).

Some average bond-distances in Ne-Ks series are shown in Figure 11. Samples used to obtain the trend lines for unit-cell parameters are the same as those used to obtain trend lines for the nepheline samples, five samples for the average <(Na,K)1-O>[7] and four samples for the average <K-O>[9] distance. The one tetrakalsilite and six kalsilite samples are grouped together and a trend line plotted for their average <(Na,K)-O>[9] distance in kalsilite (Table 4c). The one such data point for tetrakalsilite is a grand mean of the averages, where <(Na,K)-O> = 2.902 Å (Table 4b). There is a clear break between nepheline and tetrakalsilite samples at V ≈ 761 Å^3. The tetrakalsilite and the kalsilite samples fall along a straight line. The high amount of Si in series-3 samples and Ca atoms in the natural sample-1 from Monte Somma cause an increase in vacancies at the K site, so the average <K-O>[9] distance is larger than the trend lines at low V [sample-16 (Ksof = 0), sample-17 (Ksof = 0.28(4)), sample-18 (Ksof = 0.472(2)) and sample-1 (Ksof = 0.623(2))]. At low V, the series-2 Na-rich samples have average <K-O>[9] distances smaller than the trend lines because they contain fewer vacancies at the K site [sample-6 (Ksof = 0.48(3)), sample-7 (Ksof = 0.45(4)) and sample-8 (Ksof = 0.813(2))]. Simultaneously, the average <(Na,K)1-O>[7] distance is constant, as it is filled with Na atoms. The small amount of Ca atoms in sample-1 causes the

average <(Na,K)1-O>[7] to be the shortest because of the different Ca^{2+} vs. Na^{1+} cation charge. The grand mean of the <(Na,K)-O>[9] distances in tetrakalsilite and those for the six kalsilite samples fall on a linear trend line. Data for trikalsilite from Bonaccorsi et al. (1988) are also shown.

At V = 726.441(1) Å^3, Ks = 0.23 (sample-9; Tables 1, 2a), a break occurs in the average <Na1-O>[7] and <K-O>[9] bond distances for nepheline (Fig. 11). At Ks > 0.23, K atoms enter the Na1 site and the average <Na1-O>[7] distance increases because of the larger size of the K atom. At Ks < 0.23, the average <Na1-O>[7] is about constant because the Na1 site is essentially filled with Na atoms. Above V = 726.441(1) Å^3, the line representing nepheline (<(Na,K)1-O>[7]) and the second line representing tetrakalsilite and kalsilite (<(Na,K)-O>[9]) are nearly parallel as a result of a substitutional mechanism in which K replaces Na. In the case of the nepheline series, <(Na,K)1-O>[7] changes from 2.631 (sample-9) to 2.721 (sample-12b) Å, a difference of 0.090 Å. From tetrakalsilite to end-member kalsilite, the <(Na,K)-O>[9] distance changes from 2.848 to 2.932, a difference of 0.084 Å. Whereas a similar change in <K-O>[9] from 2.992 (sample-9) to 3.025 (sample-12a) takes place in nepheline, a difference of just 0.033 Å, the implication is that the average <K-O>[9] distance is affected by the percentage of vacancies and K atoms at the K site.

Sample-16 has the smallest V because it contains no K atoms, with an average <Na(K)-O>[6] = 2.799 Å. Sample-6 has the next smallest V with Ks = 0.05 and the average <K-O>[9] = 2.958 Å. Thereafter, for the next five samples with V < 726.441(1) Å^3, average <K-O>[9] values are either above or below the trend line. For V > 726.441(1) Å^3, the average <K-O>[9] increases only slightly before the last nepheline data point decreases towards tetrakalsilite. However, most of the <K-O>[9] distances in nepheline are close to 3.0 Å and any variations occur because of different amounts of K atoms and vacancies at the K site.

SUMMARY

We achieved the intended goals of this study by obtaining the crystal structures of 18 samples within the nepheline-tetrakalsilite-kalsilite series on a fine compositional scale, having found well-defined structural variations across the series that are a function of both

Na:K ratio and the presence of vacancies in various alkali sites. Moreover, with the use of mostly-synthetic samples, we have been able overcome the lack of structural variation that results from dependence on the use of natural samples, which show limited variation both in terms of Na:K ratio and vacancy content. Because natural samples plot close to samples from the so called "synthetic series," our results can indeed be applied to natural systems. Nevertheless, it would be interesting to see how the results for additional natural samples having greater diversity in compositions, if discovered, would compare to present results.

Phase transitions in minerals and their reversibility continue to intrigue researchers. Synchrotron high-resolution powder X-ray diffraction uses a highly intense beam that is sensitive to fine-scale intergrowths or overlapping multi-phases with subtle change in symmetry that cannot be resolved with conventional powder X-ray diffraction. For example, the $P31c$ to $P6_3$ transition in kalsilite may be monitored using the 111 reflection that is clearly observable with HRPXRD. Overall, the results for this project showcase the effectiveness of this experimental technique.

IMPLICATIONS

This study has shown that samples within the Ne-Ks series may contain two phases having slightly different compositions. Indeed, the tendency to form coexisting phases is perhaps not surprising, given the positive enthalpies of mixing measured for series members reported by Hovis and Roux (1993, 1999). Additionally, whereas it is common to use the electron probe microanalyzer (EPMA) to obtain chemical compositions and relate them to unit-cell parameters, we obtained good linear relations between the unit-cell volume and Ks (EPMA values) across the Ne-Ks series (Fig. 12). As a result, good compositional data can be obtained from unit-cell volume and vice versa.

K-rich nepheline and kalsilite occur in volcanic rocks because high temperatures expand the aluminosilicate framework to accommodate large K atoms. Whereas $P6_3$ kalsilite occurs in volcanic rocks, $P31c$ kalsilite occurs in lower-temperature metamorphic rocks. The high-to-low transition is not completely reversible because two different phases occur in all the kalsilite samples used in this study.

ACKNOWLEDGMENTS

Two anonymous reviewers and the technical Editor are thanked for useful comments and suggestions that helped to improve this manuscript. We thank Dr. Jacques Roux for meticulous synthesis of the Na-rich parent end members that formed the bases for two of the ion-exchange series studied here, as well as CNRS of France and the Earth Sciences Division of the U.S. National Science Foundation for financial support of previous research. HRPXRD data were collected at beamline 11-BM, Advanced Photon Source, Argonne National Laboratory. Use of the Advanced Photon Source was supported by the U. S. Department of Energy, Office of Science, Office of Basic Energy Sciences, under Contract No. DE-AC02-06CH11357. This work was supported by a Discovery Grant from the National Science and Engineering Research Council of Canada to SMA.

REFERENCES CITED

Andou, Y., and Kawahara, A. (1982) The existence of high-low inversion point of kalsilite. Mineralogical Journal, 11, 72-77.

-. (1984) The refinement of the structure of synthetic kalsilite. Mineralogical Journal, 12, 153-161.

Angel, R.J., Gatta, G.D., Boffa Ballaran, T., and Carpenter, M.A. (2008) The mechanism of coupling in the modulated structure of nepheline. Canadian Mineralogist, 46, 1465-1476.

Antao, S.M. (2013a) The mystery of birefringent garnet: is the symmetry lower than cubic? Powder Diffraction, 28, 281-288.

-. (2013b) Three cubic phases intergrown in a birefringent andradite-grossular garnet and their implications. Physics and Chemistry of Minerals, 40, 705-716.

Antao, S.M., and Hassan, I. (2010) Nepheline: structure of three samples from the Bancroft area, Ontario, obtained using synchrotron high-resolution powder X-ray diffraction. Canadian Mineralogist, 48, 69-80.

Antao, S.M., Hassan, I., Wang, J., Lee, P.L., and Toby, B.H. (2008) State-of-the-art high-resolution powder X-ray diffraction (HRPXRD) illustrated with Rietveld structure refinement of quartz, sodalite, tremolite, and meionite. Canadian Mineralogist, 46, 1501-1509.

Antao, S.M., and Klincker, A.M. (2013) Origin of birefringence in andradite from Arizona, Madagascar, and Iran. Physics and Chemistry of Minerals, 40, 575-586.

Antao, S.M., and Nicholls, J.W. (2018) Crystal chemistry of three volcanic K-rich nepheline samples from Oldoinyo Lengai, Tanzania and Mount Nyiragongo, Eastern Congo, Africa. Frontiers in Earth Science, doi: 10.3389/feart.2018.00155.

Balassone, G., Kahlenberg, V., Altomare, A., Mormone, A., Rizzi, R., Saviano, M., and Mondillo, N. (2014) Nephelines from the Somma-Vesuvius volcanic complex (Southern Italy): crystal-chemical, structural and genetic investigations. Mineralogy and Petrology, 108, 71-90.

Benedetti, E., De Gennaro, M., and Franco, E. (1977) Primo rinvenimento in natura di tetrakalsilite. Rend. Acc. Naz. Lincei Ser. VIII, 62, 835-838.

Bonaccorsi, E., Merlino, S., and Pasero, M. (1988) Trikalsilite: its structural relationships with nepheline and tetraskalsilite. Neues Jahrbuch fur Mineralogie, Monatshefte, 1988, 559-567.

Buerger, M.J., Klein, G.E., and Donnay, G. (1954) Determination of the crystal structure of nepheline. American Mineralogist, 39, 805-818.

Cagliotti, G., Paoletti, A., and Ricci, F.P. (1958) Choice of collimators for a crystal spectrometer for neutron diffraction. Nuclear Instruments, 3, 223-228.

Capobianco, C., and Carpenter, M. (1989) Thermally induced changes in kalsilite ($KAlSiO_4$). American Mineralogist, 74, 797-811.

Carpenter, M., and Cellai, D. (1996) Microstructures and high-temperature phase transitions in kalsilite. American Mineralogist, 81, 561-584.

Cellai, D., Bonazzi, P., and Carpenter, M.A. (1997) Natural kalsilite, $KAlSiO_4$, with P31*c* symmetry, crystal structure and twinning. American Mineralogist, 82, 276-279.

Cellai, D., Gesing, T.M., Wruck, B., and Carpenter, M.A. (1999) X-ray study of the trigonal-hexagonal phase transition in metamorphic kalsilite. American Mineralogist, 84, 1950-1955.

Dollase, W.A. (1970) Least-squares refinement of the structure of a plutonic nepheline. Zeitschrift für Kristallographie, 132, 27-44.

Dollase, W.A., and Freeborn, W.P. (1977) The structure of $KAlSiO_4$ with $P6_3mc$ symmetry. American Mineralogist, 62, 336-340.

Dollase, W.A., and Peacor, D.R. (1971) Si-Al ordering in nephelines. Contributions to Mineralogy and Petrology, 30, 129-134.

Dollase, W.A., and Thomas, W.M. (1978) The crystal chemistry of silica-rich, alkali-deficient nepheline. Contributions to Mineralogy and Petrology, 66, 311-318.

Foreman, N., and Peacor, D.R. (1970) Refinement of the nepheline structure at several temperatures. Zeitschrift für Kristallographie, 132, 45-70.

Friese, K., Grzechnik, A., Petříćek, V., Schönleber, A., van Smaalen, S., and Morgenroth, W. (2011) Modulated structure of nepheline. Acta Crystallographica, B67, 18-29.

Gatta, G.D., and Angel, R.J. (2007) Elastic behavior and pressure-induced structural evolution of nepheline: implications for the nature of the modulated superstructure. American Mineralogist, 92, 1446-1455.

Gatta, G.D., Angel, R.J., and Carpenter, M.A. (2010) Low-temperature behavior of natural kalsilite with $P31c$ symmetry: An in situ single-crystal X-ray diffraction study. American Mineralogist, 95, 1027-1034.

Gatta, G.D., Angel, R.J., Zhao, J., Alvaro, M., Rotiroti, N., and Carpenter, M.A. (2011) Phase stability, elastic behavior, and pressure-induced structural evolution of kalsilite: A ceramic material and high-*T*/high-*P* mineral. American Mineralogist, 96, 1363-1372.

Gregorkiewitz, M. (1984) Crystal structure and Al/Si-ordering of a synthetic nepheline. Bull. Minéral, 107, 499-509.

Hahn, T., and Buerger, M.J. (1955) The detailed structure of nepheline, $KNa_3Al_4Si_4O_{16}$. Zeitschrift für Kristallographie, 106, 308-338.

Hålenius, U., Hatert, F., Pasero, M., and Mills, S.J. (2018) IMA commission on new minerals, nomenclature and classification (CNMNC) Newsletter 42. New minerals and nomenclature modifications approved in 2018. Mineralogical Magazine, 82, 445-451.

Hamada, M., Akasaka, M., and Ohfuji, H. (2018) Crystal chemistry of K-rich nepheline in nephelinite from Hamada, Shimane Prefecture, Japan. Mineralogical Magazine, 1-25. doi:10.1180/mgm.2018.133.

Hassan, I., Antao, S.M., and Hersi, A.A. (2003) Single-crystal XRD, TEM, and thermal studies of the satellite reflections in nepheline. Canadian Mineralogist, 41, 759-783.

Hassan, I., Antao, S.M., and Parise, J.B. (2004) Sodalite: high temperature structures obtained from synchrotron radiation and Rietveld refinements. American Mineralogist, 89, 359-364.

Hayward, S.A., Pryde, A.K.A., De Dombal, R.F., Carpenter, M.A., and Dove, M.T. (2000) Rigid unit modes in disordered nepheline: a study of a displacive incommensurate phase transition. Physics and Chemistry of Minerals, 27, 285-290.

Hippler, B., and Böhm, H. (1989) Structure investigation on sodium-nephelines. Zeitschrift für Kristallographie, 187, 39-53.

Hovis, G.L., and Crelling, J.A. (2000) The effects of excess silicon on immiscibility in the nepheline-kalsilite system. American Journal of Science, 300, 238-249.

Hovis, G.L., Mott, A., and Roux, J. (2009) Thermodynamic, phase equilibrium, and crystal chemical behaviour in the nepheline-kalsilite system. American Journal of Science, 309, 397-419.

Hovis, G.L., and Roux, J. (1993) Thermodynamic mixing properties of nepheline-kalsilite crystalline, solutions. American Journal of Science, 293, 1108-1127.

-. (1999) Thermodynamics of excess silicon in nepheline and kalsilite crystalline solutions. European Journal of Mineralogy, 11, 815-827.

Hovis, G.L., Spearing, D.R., Stebbins, J.F., Roux, J., and Clare, A. (1992) X-ray powder diffraction and ^{23}Na, ^{27}Al, and ^{29}Si MAS-NMR investigation of nepheline-kalsilite crystalline solutions. American Mineralogist, 77, 19-29.

Kawahara, A., Andou, Y., Marumo, F., and Okuno, M. (1987) The crystal structure of high temperature form of kalsilite ($KAlSiO_4$) at 950 °C. Mineralogical Journal, 13, 260-270.

Kremenović, A., Lazic, B., Krüger, H., Tribus, M., and Vulić, P. (2013) Monoclinic structure and nonstoichiometry of '$KAlSiO_4$-O1'. Acta Crystallographica, C69, 334-336.

Kremenović, A., and Vulić, P. (2014) Disordered kalsilite $KAlSiO_4$. Acta Crystallographica, C70, 256-259.

Larson, A.C., and Von Dreele, R.B. (2000) General Structure Analysis System (GSAS). Los Alamos National Laboratory Report, LAUR 86-748.

Lee, P.L., Shu, D., Ramanathan, M., Preissner, C., Wang, J., Beno, M.A., Von Dreele, R.B., Ribaud, L., Kurtz, C., Antao, S.M., Jiao, X., and Toby, B.H. (2008) A twelve-analyzer detector system for high-resolution powder diffraction. Journal of Synchrotron Radiation, 15, 427-432.

McConnell, J.D.C. (1962) Electron-diffraction study of subsidiary maxima of scattered intensity in nepheline. Mineralogical Magazine, 33, 114-125.

-. (1981) Time-temperature study of the intensity of satellite reflections in nepheline. American Mineralogist, 66, 990-996.

-. (1991) Incommensurate structures. Philosophical Transactions of the Royal Soc. London, A334, 425-437.

Merlino, S. (1984) Feldspathoids: their average and real structures. In W.L. Brown, Ed. Feldspars and Feldspathoids, Nato ASI Series C, 137, 435-470, D. Reidel Publishing Company.

Merlino, S., Franco, E., Mattia, C.A., Pasero, M., and De Gennaro, M. (1985) The crystal structure of panunzite (natural tetrakalsilite). Neues Jahrb. Mineral., Mh., 1985, 322-328.

Palmer, D.C. (1994) Stuffed derivatives of the silica polymorphs. Rev. Min., 29, 83-122.

Parker, J.M. (1972) The domain structure of nepheline. Zeitschrift für Kristallographie, 136, 255-272.

Parker, J.M., and McConnell, J.D.C. (1971) Transformation behaviour in the mineral nepheline. Nature 234, 178-179.

Perrotta, A.J., and Smith, J.V. (1965) The crystal structure of kalsilite $KAlSiO_4$. Mineralogical Magazine, 35, 588-595.

Rietveld, H.M. (1969) A profile refinement method for nuclear and magnetic structures. Journal of Applied Crystallography, 2, 65-71.

Rossi, G., Oberti, R., and Smith, D.C. (1989) The crystal structure of a K-poor, Ca-rich silicate with the nepheline framework and crystal chemical relationships in the compositional space $(K,Na,Ca,[])_8(Al,Si)_{16}O_{32}$. European Journal of Mineralogy, 1, 59-70.

Sahama, T.G. (1958) A complex form of natural nepheline form Iivaara, Finland. American Mineralogist, 43, 165-166.

-. (1962) Order-disorder in natural nepheline solid solutions. Journal of Petrology, 3, 65-81.

Schiebold, E. (1930) Zur Strucktur von Nepheline and Analcim. Naturwissenschaften, 1S, 705-706.

Simmons, W.B., and Peacor, D.R. (1972) Refinement of the crystal structure of a volcanic nepheline. American Mineralogist, 57, 1711-1719.

Tait, K.T., Sokolova, E., Hawthorne, F.C., and Khomyakov, A.P. (2003) The crystal chemistry of nepheline. Canadian Mineralogist, 41, 61-70.

Thompson, P., Cox, D.E., and Hastings, J.B. (1987) Rietveld refinement of Debye-Scherrer synchrotron X-ray data from alumina. Journal of Applied Crystallography, 20, 79-83.

Toby, B.H. (2001) EXPGUI, a graphical user interface for GSAS. Journal of Applied Crystallography, 34, 210-213.

Tuttle, O.F., and Smith, J.V. (1958) The nepheline-kalsilite system II: phase relations. American Journal of Science, 256, 571-589.

Uchida, H., Downs, R.T., and Yang, H. (2006) Crystal-chemical investigation of kalsilite from San Venanzo, Italy, using single-crystal X-ray diffraction and Raman spectroscopy. Geochmica et Cosmochimica Acta, 70, A677.

Vulić, R., Balić-Žunić, T., Belmonte, L.J., and Kahlenberg, V. (2011) Crystal chemistry of nephelines from ijolites and nepheline-rich pegmatites: influence of composition and genesis on the crystal structure investigated by X-ray diffraction. Mineralogy and Petrology, 101, 185-194.

Wang, J., Toby, B.H., Lee, P.L., Ribaud, L., Antao, S.M., Kurtz, C., Ramanathan, M., Von Dreele, R.B., and Beno, M.A. (2008) A dedicated powder diffraction beamline at the advanced photon source: commissioning and early operational results. Review of Scientific Instruments, 79, 085105.

Xu, H., and Veblen, D.R. (1996) Superstructures and domain structures in natural and synthetic kalsilite. American Mineralogist, 81, 1360-1370.

Endnote:

[1]Deposit item AM-XX-XXXXX, Tables 2, 3, 4 and CIFs. Deposit items are free to all readers and found on the MSA website, via the specific issue's Table of Contents (go to http://www.minsocam.org/MSA/AmMin/TOC/2020/July2020_data/Jul2020_data.html).

This is the peer-reviewed, final accepted version for American Mineralogist, published by the Mineralogical Society of America.
The published version is subject to change. Cite as Authors (Year) Title. American Mineralogist, in press.
DOI: https://doi.org/10.2138/am-2021-7484. http://www.minsocam.org/

TABLE 1. Chemical compositions compared to that obtained by Rietveld refinements for 19 samples from the Ne-Ks series

		Chemical Composition	From Chemical Formulae (*sofs*)				From Rietveld Refinement (*sofs*)			
#	No.		Ks	Na(K) site	K site	Na1 site	Ks	Na(K) site	K site	Na1 site
		"Natural" Series-1 (Hovis et al. 1992)		Na	K	Na + K/Ca = 1		Na	K	Na + K/Ca = 1
1	8311	$(K_{0.129}Na_{0.747}Ca_{0.036}\square_{0.088})_{\Sigma1}[Al_{0.948}Si_{1.052}O_4]$	0.129	0.044	0.516	0.952Na + 0.048Ca	0.156	---	0.623(2)	0.972(2) Na+0.028(2) Ca
2	8928	$(K_{0.672}Na_{0.252}Ca_{0.013}\square_{0.064})_{\Sigma1}[Al_{0.949}Si_{1.051}O_4]$	0.672	---	---	complex	?	---	---	Not refined (Tetra-Ks)
3a	8807	$(K_{0.736}Na_{0.193}Ca_{0.010}\square_{0.062})_{\Sigma1}[Al_{0.948}Si_{1.052}O_4]$	0.736	---	---	$(K_{0.736}Na_{0.193}Ca_{0.010})$	0.791(5)	---	---	0.791(5) K + 0.157(5) Na
3b			0.736	---	---	$(K_{0.736}Na_{0.193}Ca_{0.010})$	0.90(2)	---	---	0.90(2) K + 0.05(2) Na
4a	8719	$(K_{0.937}Na_{0.008}Ca_{0.002}\square_{0.053})_{\Sigma1}[Al_{0.948}Si_{1.052}O_4]$	0.937	---	---	$(K_{0.937}Na_{0.008}Ca_{0.002})$	1	---	---	1 K
4b			0.937	---	---	$(K_{0.937}Na_{0.008}Ca_{0.002})$	0.935(1)	---	---	0.935(1) K
5a	8860	$(K_{0.948}\square_{0.052})_{\Sigma1}[Al_{0.948}Si_{1.052}O_4]$	0.948	---	---	0.948 K	1	---	---	1 K
5b			0.948	---	---	0.948 K	0.950(2)	---	---	0.950(2)
		"Synthetic" Series-2 (Hovis et al. 1992)						---		
6	880408	$(K_{0.050}Na_{0.933}\square_{0.017})_{\Sigma1}[Al_{0.983}Si_{1.017}O_4]$	0.050	0.244	0.200	1 Na	0.120	0.09(1)	0.48(3)	1 Na
7	8824	$(K_{0.108}Na_{0.875}\square_{0.017})_{\Sigma1}[Al_{0.983}Si_{1.017}O_4]$	0.108	0.167	0.432	1 Na	0.112	0.17(2)	0.45(4)	1 Na
8	8825	$(K_{0.162}Na_{0.821}\square_{0.017})_{\Sigma1}[Al_{0.983}Si_{1.017}O_4]$	0.162	0.095	0.648	1 Na	0.203	---	0.813(2)	1 Na
9	8826	$(K_{0.218}Na_{0.765}\square_{0.017})_{\Sigma1}[Al_{0.983}Si_{1.017}O_4]$	0.218	0.020	0.872	1 Na	0.228	---	0.912(1)	1 Na
10	8827	$(K_{0.315}Na_{0.668}\square_{0.017})_{\Sigma1}[Al_{0.983}Si_{1.017}O_4]$	0.315	---	0.932	0.109 K + 0.891 Na	0.349	---	0.957(1)	0.15(1) K + 0.81(2) Na
11	8834	$(K_{0.409}Na_{0.574}\square_{0.017})_{\Sigma1}[Al_{0.983}Si_{1.017}O_4]$	0.409	---	0.932	0.235 K + 0.765 Na	0.390	---	0.959(2)	0.200(2) K + 0.800(2) Na
12a	8853	$(K_{0.499}Na_{0.484}\square_{0.017})_{\Sigma1}[Al_{0.983}Si_{1.017}O_4]$	0.499	---	0.932	0.355 K + 0.645 Na	0.466	---	0.960(2)	0.301(3) K + 0.699(3) Na
12b	8853	?	?				0.567	---	0.930(6)	0.446(9) K + 0.554(9) Na
13	8843	$(K_{0.698}Na_{0.285}\square_{0.017})_{\Sigma1}[Al_{0.983}Si_{1.017}O_4]$	0.698	---	---	complex	0.666	---	---	See Table 3b (Tetra-Ks)
14a	8828	$(K_{0.790}Na_{0.193}\square_{0.017})_{\Sigma1}[Al_{0.983}Si_{1.017}O_4]$	0.790	---	---	$(K_{0.790}Na_{0.193})$	0.798(2)	---	---	0.798(2) K + 0.185(2) Na
14b			0.790	---	---	$(K_{0.790}Na_{0.193})$	1	---	---	1 K
15a	8823	$(K_{0.983}\square_{0.017})_{\Sigma1}[Al_{0.983}Si_{1.017}O_4]$	0.983	---	---	0.983 K	1	---	---	1 K
15b			0.983	---	---	0.983 K	0.966(2)	---	---	0.966(2) K
		"High-Si" Series-3 (Hovis and Roux 1999; Hovis et al. 2009)								
16	9504	$(K_{0.0}Na_{0.875}\square_{0.125})_{\Sigma1}[Al_{0.875}Si_{1.125}O_4]$	0	0.167	---	1 Na	0	0.178(1)	---	1 Na
17	9514	$(K_{0.052}Na_{0.823}\square_{0.125})_{\Sigma1}[Al_{0.875}Si_{1.125}O_4]$	0.052	0.097	0.208	1 Na	0.070	0.07(2)	0.28(4)	1 Na
18	9508	$(K_{0.101}Na_{0.774}\square_{0.125})_{\Sigma1}[Al_{0.875}Si_{1.125}O_4]$	0.101	0.032	0.404	1 Na	0.118	---	0.472(2)	1 Na
19a	9507	$(K_{0.875}Na_{0.0}\square_{0.125})_{\Sigma1}[Al_{0.875}Si_{1.125}O_4]$	0.875			0.875 K	0.870(5)	---	---	0.870(5) K
19b			0.875			0.875 K	0.966(2)	---	---	0.966(2) K

Kalsilite samples contain a mixture of $P6_3$ (3a, 4a, etc.) and $P31c$ phases (3b, 4b, etc.). Sample 12 is a mixture of two different nepheline phases (12a and 12b).

This is the peer-reviewed, final accepted version for American Mineralogist, published by the Mineralogical Society of America.
The published version is subject to change. Cite as Authors (Year) Title. American Mineralogist, in press.
DOI: https://doi.org/10.2138/am-2021-7484. http://www.minsocam.org/

List of Figures

FIGURE 1. (*a*) Crystal structure of nepheline projected down the **c** axis (a_1 is horizontal and a_2 is 120° away from a_1; a hexagonal unit-cell is outlined with a solid line). The K site (yellow) on the 6_3 axis in the hexagonal channels contains K atoms and vacancies. The Na1 site in the oval-shaped channels contains mainly Na atoms (blue), minor Ca atoms, and K atoms in K-rich samples. In Na-rich nepheline (with small amounts of K atoms), the Na atoms are disordered around the 6_3 axis at a Na(K) site (red) to form proper bonds to the O atoms (black). The K and Na(K) sites are close to each other. The tetrahedral Al and Si sites are labeled. The O1 atoms are positionally disordered (pink) in nepheline and kalsilite structures. (*b*) The 8-fold coordination of the Na1 site (blue) in nepheline by O atoms (O1 is pink, others are grey). (*c*) The 9-fold coordination of the K site (yellow) in nepheline. In Na-rich nepheline, the Na atoms are positionally disordered off the 6_3 axis at a Na(K) site (red). The coordination of the Na atom at the Na(K) site is not shown.

FIGURE 2. (*a*) Structure of kalsilite projected down the **c** axis (a_1 is horizontal and a_2 is 120° away from a_1; multiple hexagonal unit-cells are outlined with dashed lines to show the resemblance to the structures of nepheline and tetrakalsilite). A layer of alternating AlO_4 and SiO_4 tetrahedra is shown where AlO_4 (green) tetrahedra point upwards and SiO_4 (grey) tetrahedra point downwards. The O2 sites are shown as black spheres in (*a*) and grey in (*b*). The O1 site (pink) is disordered over three nearby positions, similar to the O1 site in nepheline. K atoms (yellow) are in ditrigonal rings that are "pointed" in one direction. (*b*) The 9-fold coordination of the K site in kalsilite sample-14a has average <(Na,K)-O>[9] = 2.963 Å (Table 4c).

FIGURE 3. Structure of tetrakalsilite projected down the **c** axis (a_1 is horizontal and a_2 is 120° away from a_1; a hexagonal unit-cell is outlined with a solid line). A layer of alternating AlO_4 and SiO_4 tetrahedra is shown where the AlO_4 (green) tetrahedra point downwards and the SiO_4 (grey) tetrahedra point upwards. K1 and K3 sites are in ditrigonal rings, K5 sites are in hexagonal rings, and K2, K4, and Na (blue) sites occupy oval-shaped rings. The K sites are labelled.

FIGURE 4. Full HRPXRD traces for the three Na-rich nepheline samples: (a) sample-16, (b) sample-8, and (c) sample-1. Calculated (continuous) and observed (crosses) profiles are shown. The difference curve ($I_{obs} - I_{calc}$) is shown at the bottom. The short vertical lines indicate the allowed reflection positions. The

This is the peer-reviewed, final accepted version for American Mineralogist, published by the Mineralogical Society of America.
The published version is subject to change. Cite as Authors (Year) Title. American Mineralogist, in press.
DOI: https://doi.org/10.2138/am-2021-7484. http://www.minsocam.org/

intensities for the trace and difference curve that are above 20° and 30° 2θ are multiplied by 5 and 10, respectively.

FIGURE 5. Expanded HRPXRD traces for three nepheline samples: (a) sample-16, (b) sample-6, and (c) sample-1. Miller indices are given for the subcell in (c) (no bars on any index). Some satellite reflections are contained in the natural sample-1 from Monte Somma; these reflections are unmarked and are not fitted, *e.g.*, between 010 and 011, and between 012 and 120 reflections.

FIGURE 6. Comparison of HRPXRD traces for four samples: (a) nepheline sample-8, (b) a two-phase nepheline sample-12, (c) tetrakalsilite sample-13, and (d) kalsilite sample-15. Nepheline sample-8 contains no impurity peaks or satellite reflections. Nepheline sample-12 contains two different nepheline phases (12a = 79.6(2) and 12b = 20.4(5) wt. %). The tetrakalsilite sample-13 contains some satellite reflections. Inserts show an expanded part of the traces. Differences occur between the four traces for the three different structures.

FIGURE 7. Expanded HRPXRD traces from 7.4 to 11.2° 2θ for six kalsilite samples. Calculated (continuous) and observed (crosses) profiles are shown. The difference curve ($I_{obs} - I_{calc}$) is shown at the bottom. The short vertical lines indicate the allowed reflection positions. All six samples contain two kalsilite phases with space groups $P6_3$ and $P31c$. The 012 reflection represents the 100 % peak. From (*a*) to (*f*), the wt. % of the $P6_3$ kalsilite phase decreases from 99.33(1) % to 22.2(1) %. This is also reflected in the intensities of the 111 reflections that decrease from (*a*) to (*f*). All the reflections including the 111 reflection in (*f*) are broad, compared to the other samples. As the 111 intensity decreases, the 112 intensity tends to increase indicating an increasing amount of the $P31c$ kalsilite phase (the 112 reflections overlap in both phases). Weak unfitted satellite reflection are present in (*b*), (*e*), and (*f*); these are easily observed in the difference curves.

FIGURE 8. Linear trends among unit-cell parameters for Ne-Ks series meet at tetrakalsilite (circled points). The linear *a vs*. *V* plot in (*a*) shows very little scatter, followed by *c vs. V* in (b), and *c*/*a vs*. *V* in (*c*) that shows the most scatter. The "high-Si" series-3 data points deviate (smaller *c* and *c/a* parameters) the most from the trend lines because of excess amounts of small Si compared to Al atoms [sample-19 is excluded from the trend-line computation]. Literature sources are given in the text. The *a* unit-cell values shown for kalsilite are doubled and those for tetrakalsilite are halved.

FIGURE 9. Linear trends between *c* and *a* unit-cell parameters for Ne-Ks series that meet at tetrakalsilite (circled points). High-Si series-3 samples deviate the most from the trend lines because of excess Si atoms [sample-19 is excluded from the trend-line computation]. Literature sources are given in the text. The *a* unit-cell values shown for kalsilite are doubled and those for tetrakalsilite are halved.

FIGURE 10. Difference Fourier maps for three Na-rich nepheline samples: (*a*) sample-16, (*b*) sample-6, and (*c*) sample-1 showing the electron density after the Na(K) and K sites were removed from the structural models. The Na(K) site is off the 6_3 axis in (*a*) and (*b*). The K site is on the 6_3 axis in (*b*) and (*c*). The contour intervals are 0.4 in (*a*) and 1.0 in (*b*) and (*c*).

FIGURE 11. Structural variations across Ne-Ks series. Four samples contain Na atoms at the Na(K) site (triangles) and sample-16 contains no K atoms. Seven Na-rich nepheline samples are above or below the average <K-O>[9] trend line because of vacancies at the K site. These seven samples have the smallest *V*. The high amount of Si in series-3 samples causes an increase in vacancies at the K site, so the average <K-O>[9] distance is larger than the trend lines at low *V*. Simultaneously, the average <(Na,K)1-O>[7] is constant, as the Na1 site is filled only with Na atoms in these seven samples. Sample-1 from Monte Somma contains some Ca atoms and 5.2 mole % excess Si; both cause vacancies at the K site and a contraction in the <(Na,K)1-O>[7] distance, which is the smallest distance because Ca atoms occur at the Na1 site. The grand mean of the average <(Na,K)-O> distances in tetrakalsilite (circled data point) is shown. The trend lines were calculated using the data points shown as circles with + in the centre.

FIGURE 12. Three linear lines are used to represent the relation between the *V* unit-cell parameter and Ks (EPMA values) across the Ne-Ks series. From the unit-cell volume, good compositional data can be obtained with the inserted equations. The *a* unit-cell values for kalsilite are doubled and those for tetrakalsilite are halved, and the *V* is calculated. Data for samples-13 and -19 are omitted.

This is the peer-reviewed, final accepted version for American Mineralogist, published by the Mineralogical Society of America.
The published version is subject to change. Cite as Authors (Year) Title. American Mineralogist, in press.
DOI: https://doi.org/10.2138/am-2021-7484. http://www.minsocam.org/

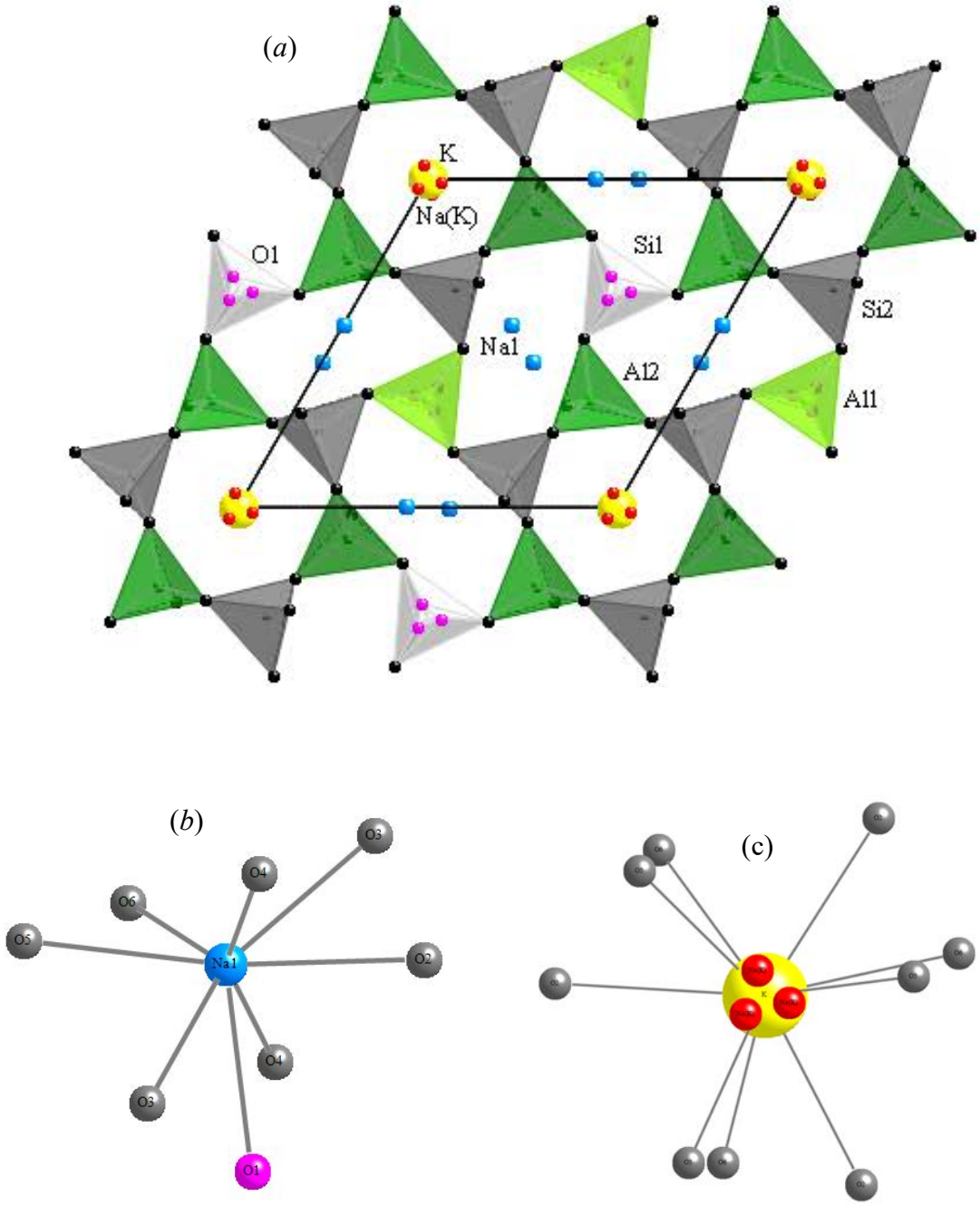

Fig. 1

This is the peer-reviewed, final accepted version for American Mineralogist, published by the Mineralogical Society of America.
The published version is subject to change. Cite as Authors (Year) Title. American Mineralogist, in press.
DOI: https://doi.org/10.2138/am-2021-7484. http://www.minsocam.org/

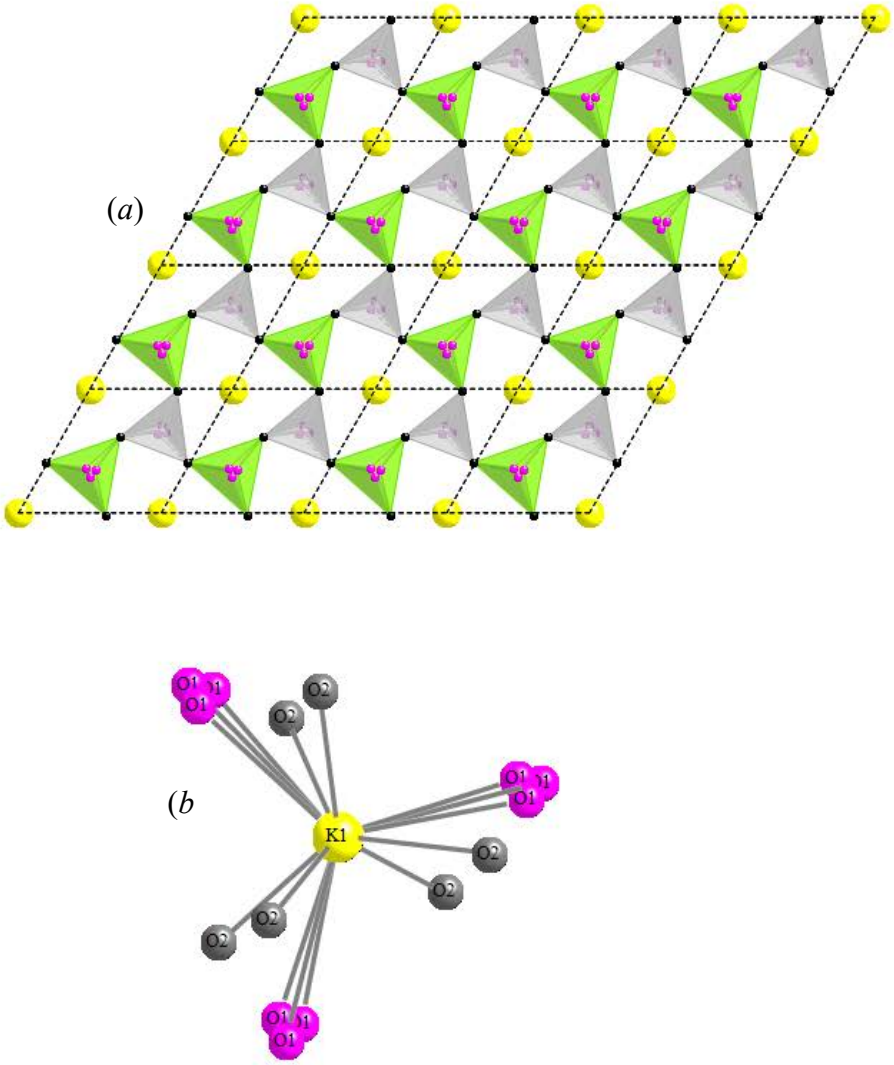

Fig. 2

This is the peer-reviewed, final accepted version for American Mineralogist, published by the Mineralogical Society of America.
The published version is subject to change. Cite as Authors (Year) Title. American Mineralogist, in press.
DOI: https://doi.org/10.2138/am-2021-7484. http://www.minsocam.org/

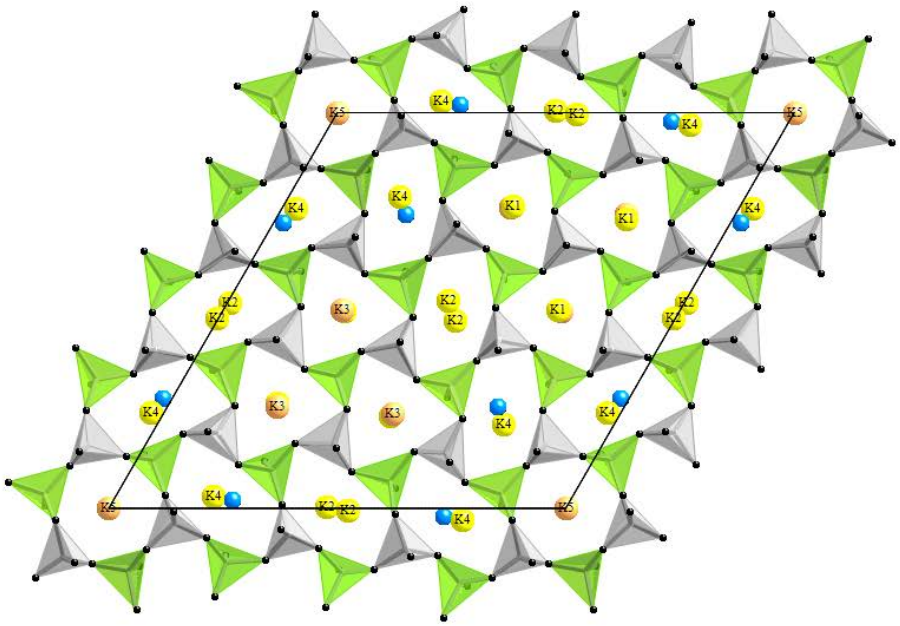

Fig. 3

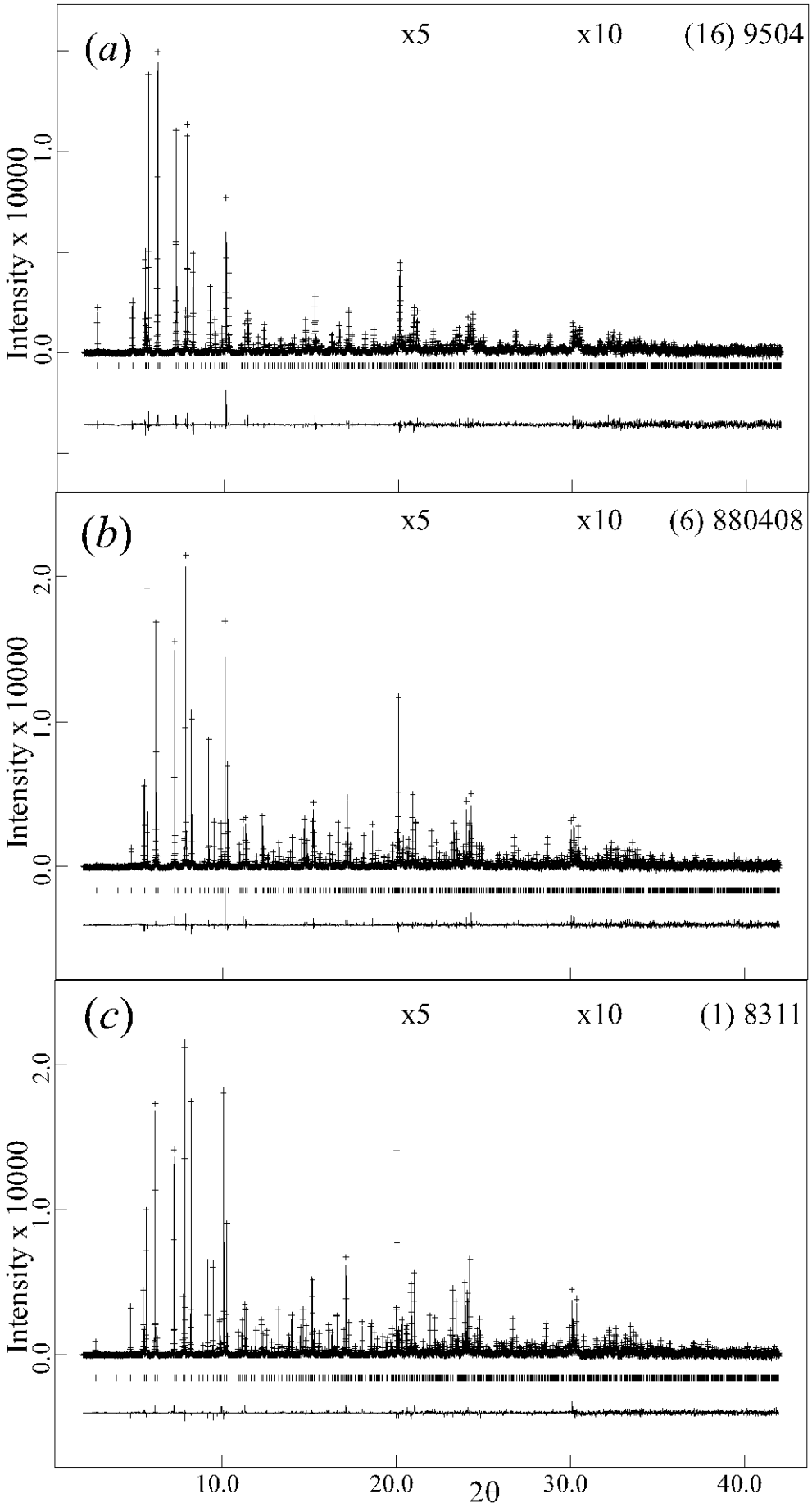

Fig. 4

This is the peer-reviewed, final accepted version for American Mineralogist, published by the Mineralogical Society of America.
The published version is subject to change. Cite as Authors (Year) Title. American Mineralogist, in press.
DOI: https://doi.org/10.2138/am-2021-7484. http://www.minsocam.org/

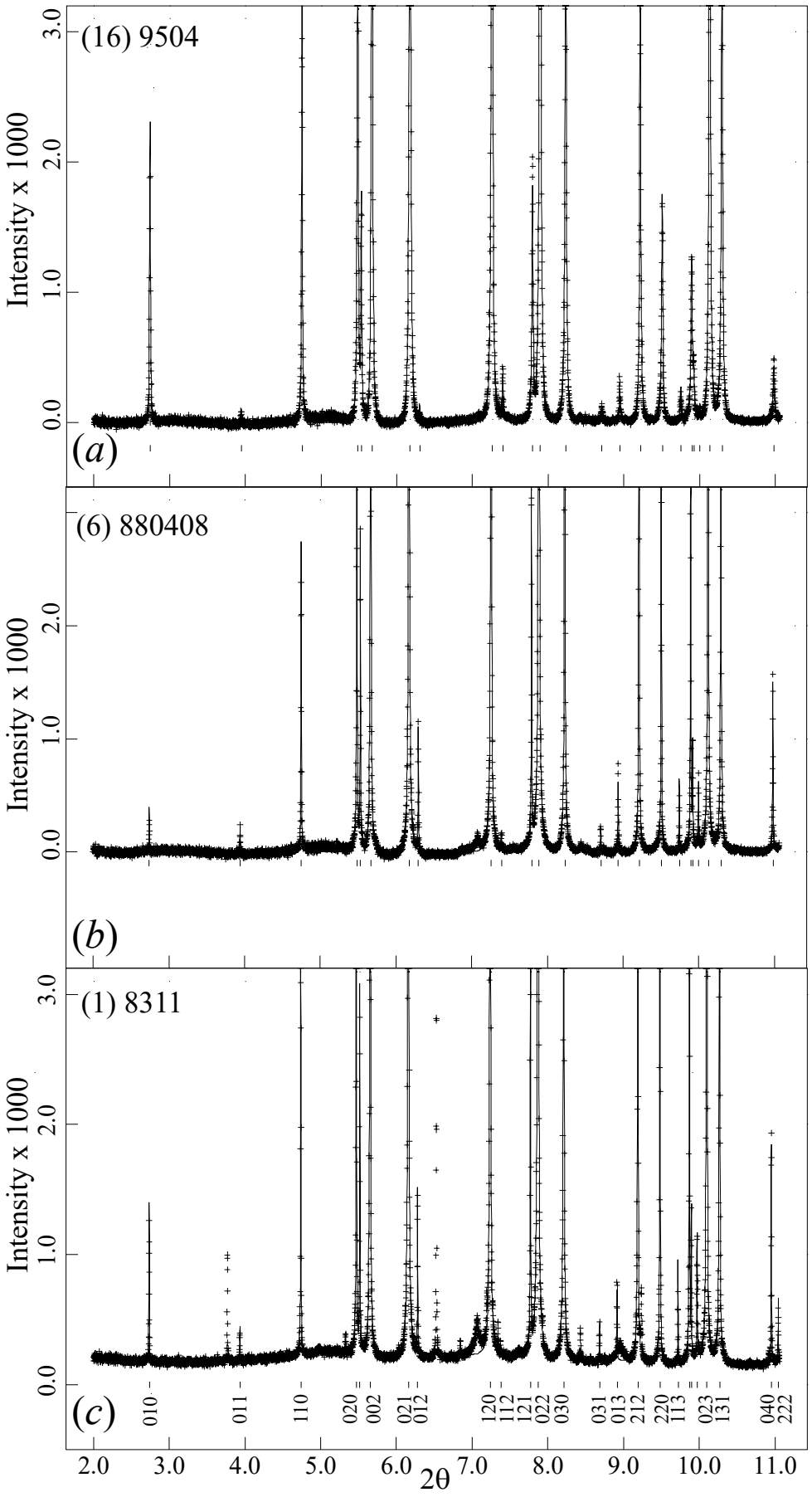

Fig. 5

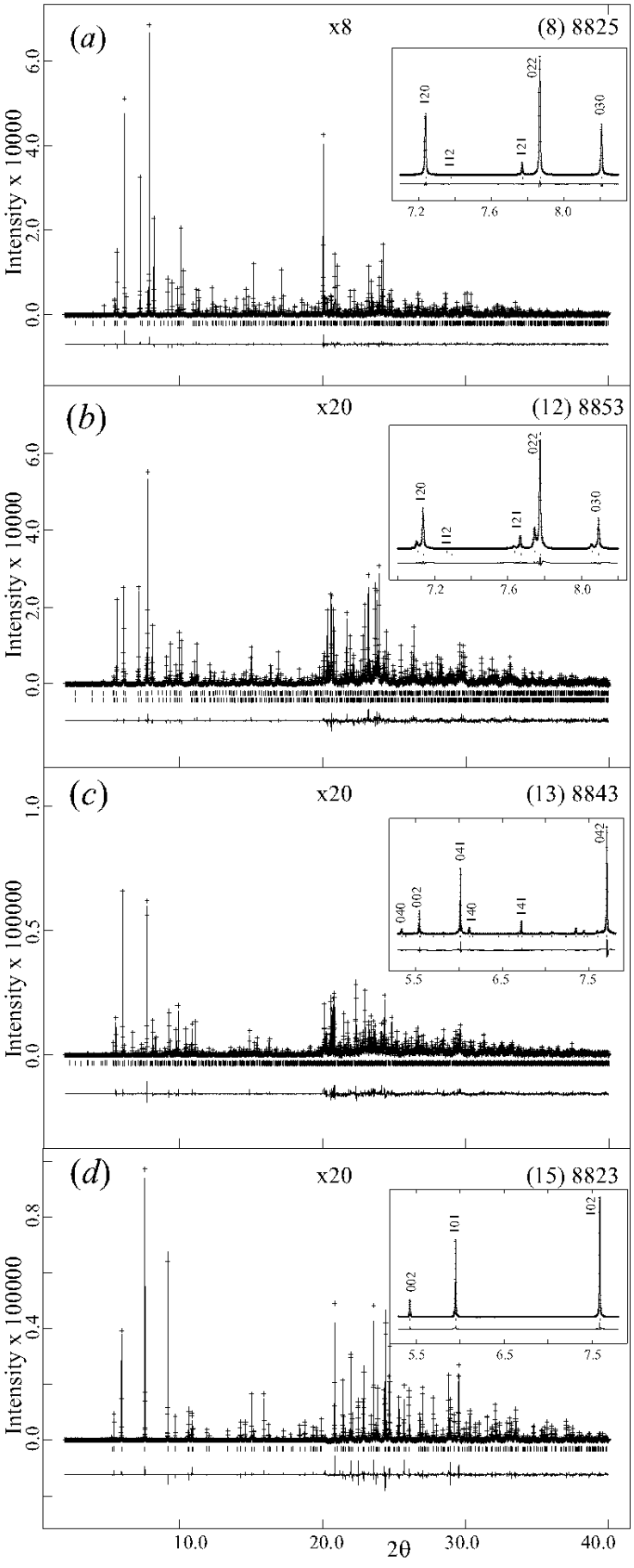

Fig. 6

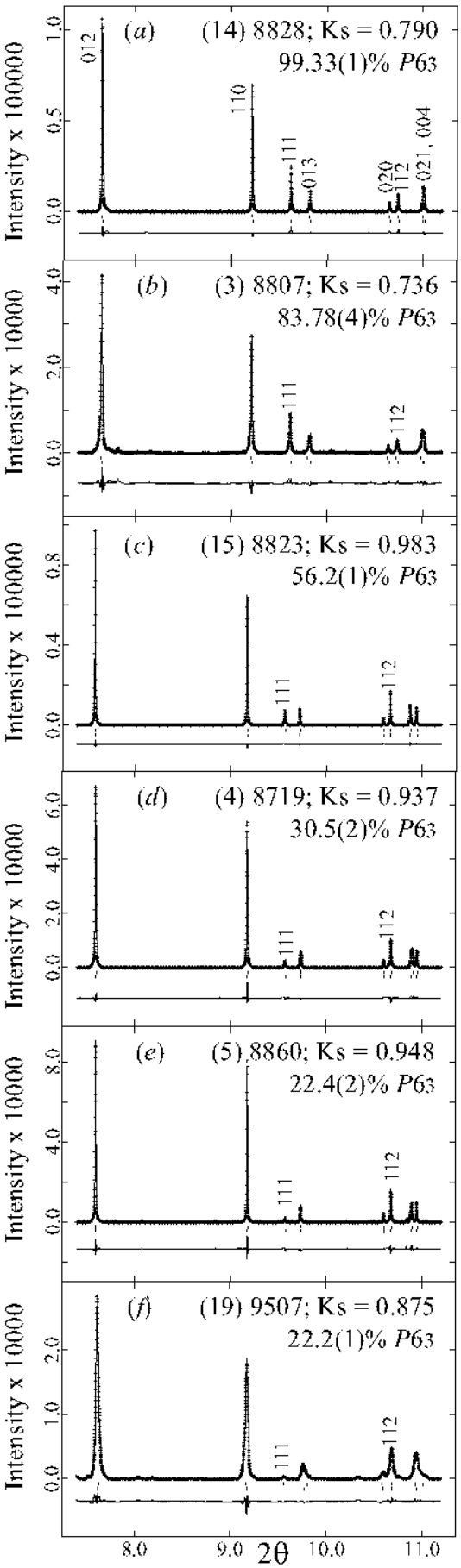

Fig. 7

This is the peer-reviewed, final accepted version for American Mineralogist, published by the Mineralogical Society of America.
The published version is subject to change. Cite as Authors (Year) Title. American Mineralogist, in press.
DOI: https://doi.org/10.2138/am-2021-7484. http://www.minsocam.org/

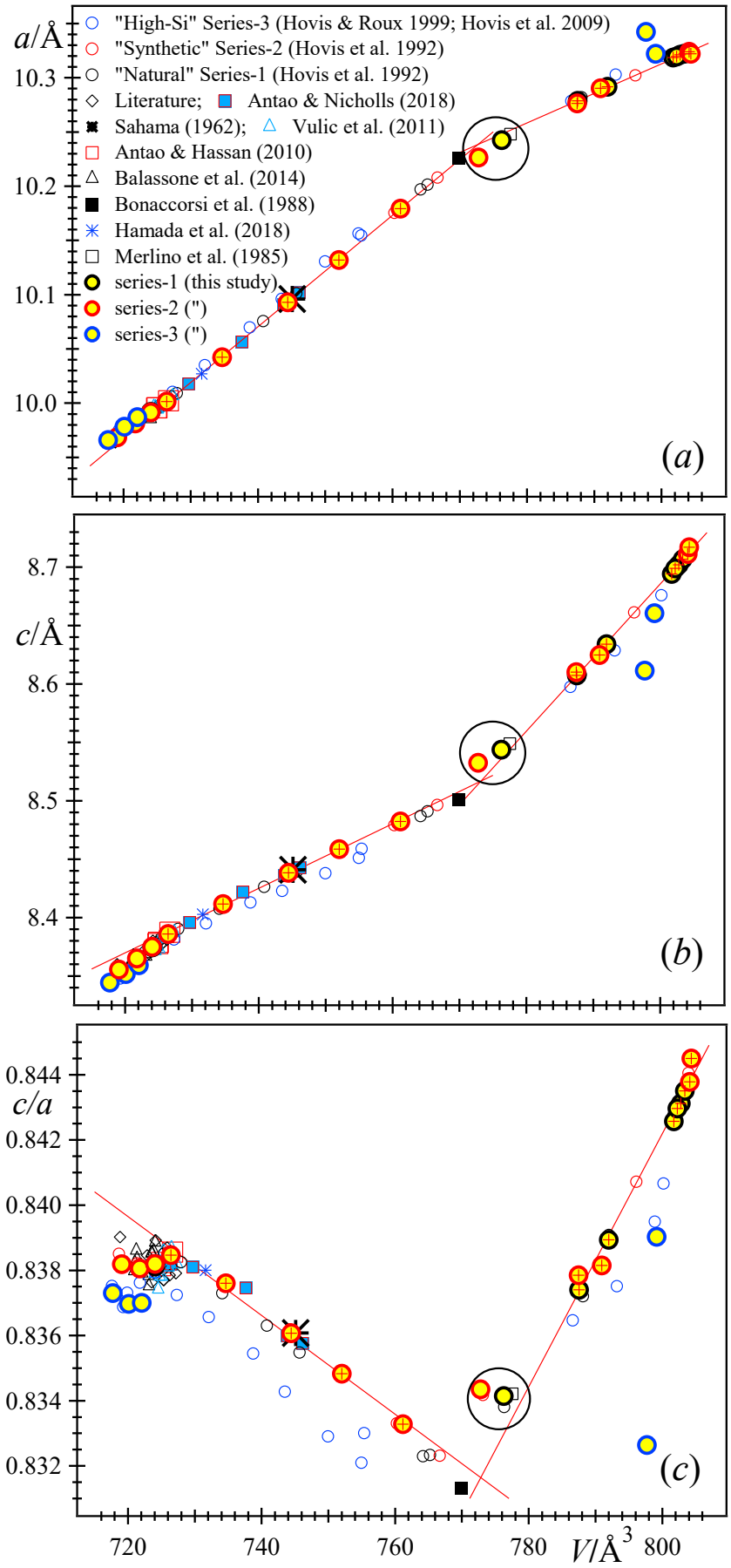

Fig. 8

This is the peer-reviewed, final accepted version for American Mineralogist, published by the Mineralogical Society of America.
The published version is subject to change. Cite as Authors (Year) Title. American Mineralogist, in press.
DOI: https://doi.org/10.2138/am-2021-7484. http://www.minsocam.org/

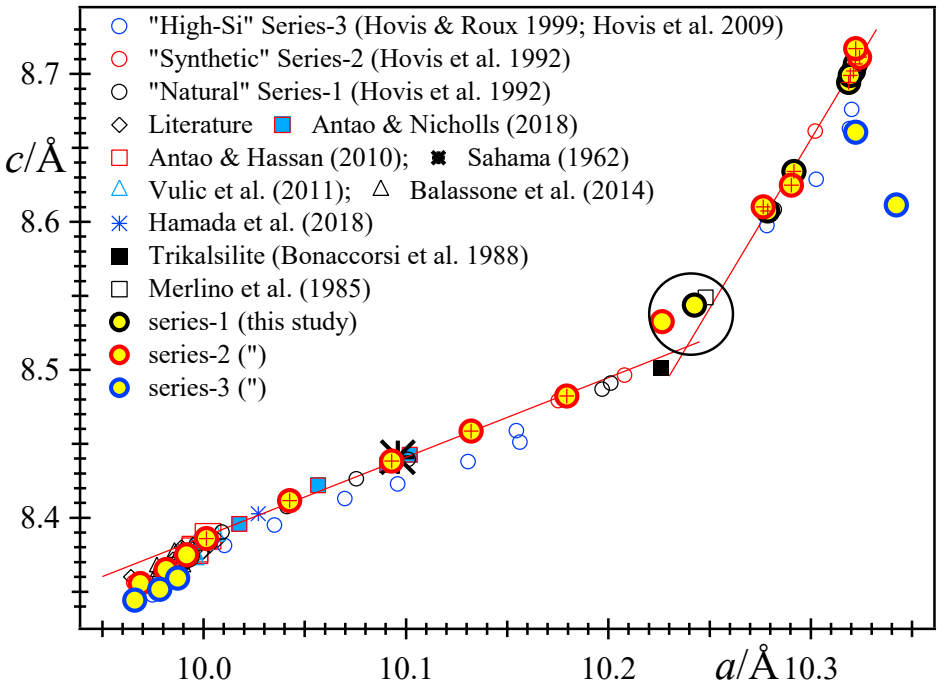

Fig. 9

This is the peer-reviewed, final accepted version for American Mineralogist, published by the Mineralogical Society of America.
The published version is subject to change. Cite as Authors (Year) Title. American Mineralogist, in press.
DOI: https://doi.org/10.2138/am-2021-7484. http://www.minsocam.org/

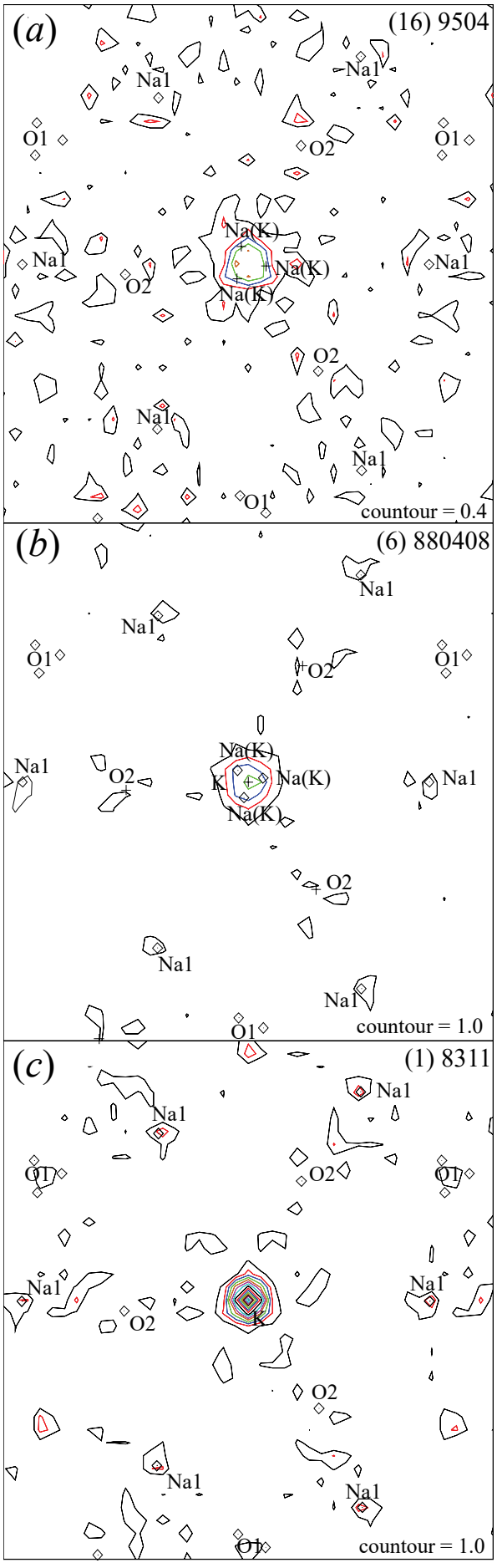

Fig. 10

This is the peer-reviewed, final accepted version for American Mineralogist, published by the Mineralogical Society of America.
The published version is subject to change. Cite as Authors (Year) Title. American Mineralogist, in press.
DOI: https://doi.org/10.2138/am-2021-7484. http://www.minsocam.org/

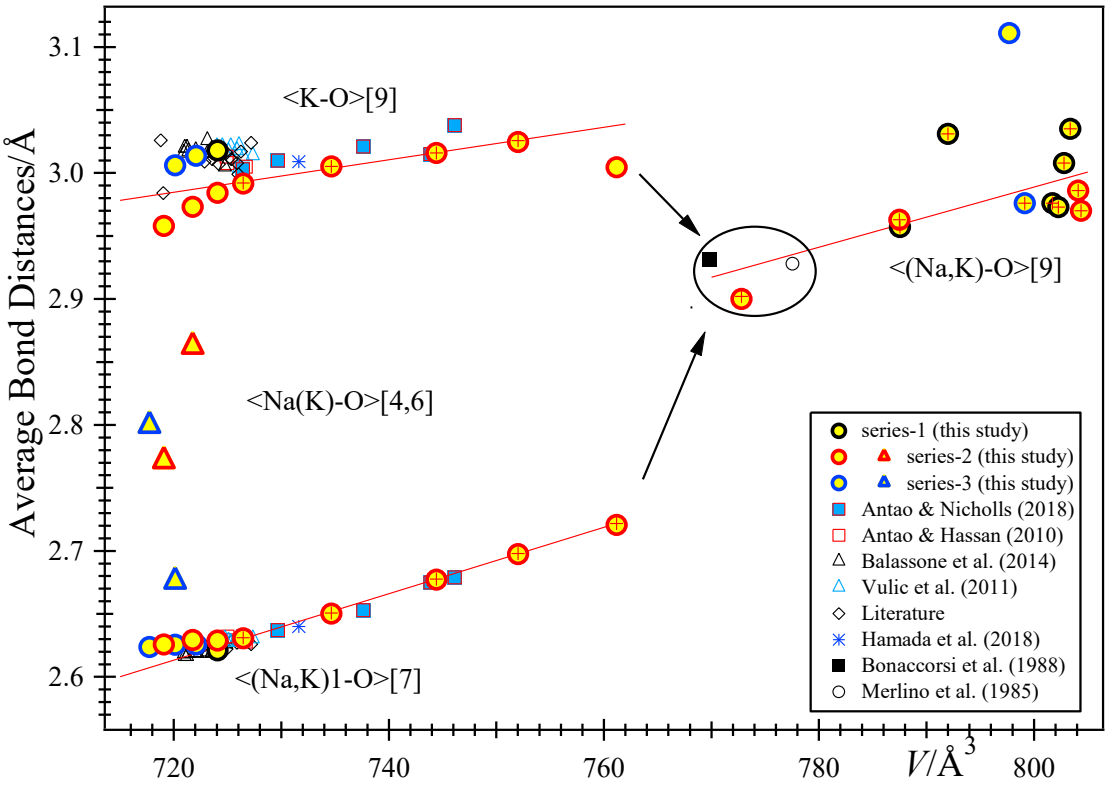

Fig. 11

This is the peer-reviewed, final accepted version for American Mineralogist, published by the Mineralogical Society of America.
The published version is subject to change. Cite as Authors (Year) Title. American Mineralogist, in press.
DOI: https://doi.org/10.2138/am-2021-7484. http://www.minsocam.org/

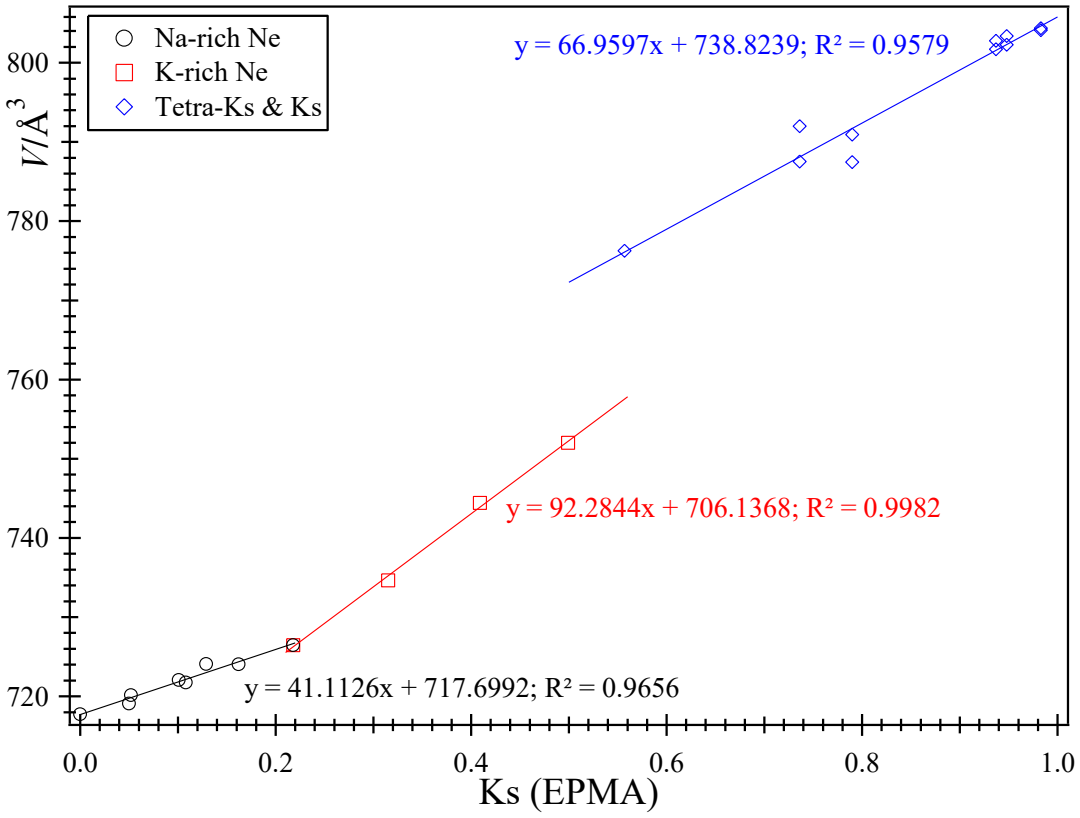

Fig. 12

Deposited Tables 2, 3, and 4

This is the peer-reviewed, final accepted version for American Mineralogist, published by the Mineralogical Society of America.
The published version is subject to change. Cite as Authors (Year) Title. American Mineralogist, in press.
DOI: https://doi.org/10.2138/am-2021-7484. http://www.minsocam.org/

TABLE 2a. Unit-cell and Rietveld-refinement parameters for 11 nepheline and two tetrakalsilite (2, 13) samples

	1	2	**6**	**7**	**8**	**9**	**10**
	8311	8928	880408	8824	8825	8826	8827
Ks†	0.129	0.672	0.050	0.108	0.162	0.218	0.315
Ks(ref)‡	0.156	---	0.120	0.112	0.203	0.228	0.349
χ^2	1.777		1.495	1.492	1.674	1.811	1.593
R_F^2	0.0695		0.0581	0.057	0.0583	0.0523	0.0424
N_{obs}	1387		1394	1236	1240	1247	1278
# Var.*	55		55	55	55	55	55
a (Å)	9.99188(1)	20.4851(4)	9.96864(1)	9.98141(1)	9.99151(1)	10.00140(1)	10.04242(1)
c (Å)	8.37442(1)	8.5438(2)	8.35559(1)	8.36505(1)	8.37489(1)	8.38588(1)	8.41156(1)
V (Å^3)	724.069(1)	3104.97(9)	719.084(1)	721.743(1)	724.056(1)	726.441(1)	734.655(1)

	11	**12a**	**12b**	**13**	16	17	18
	8834	8853	8853	8843	9504	9514	9508
Ks	0.409	0.499	?	0.698	0	0.052	0.101
Ks(ref)	0.390	0.466	0.567	0.666	0	0.070	0.118
χ^2	2.306	2.936		10.16	1.597	2.28	2.65
R_F^2	0.0401	0.0639		0.1102	0.0457	0.0448	0.0444
N_{obs}	1314	2650		5229	1311	1298	1244
# Var.	55	89		137	55	55	55
a (Å)	10.09290(1)	10.13206(1)	10.17941(3)	20.45307(4)	9.96589(2)	9.97830(3)	9.98709(3)
c (Å)	8.43839(1)	8.45854(1)	8.48229(4)	8.53254(2)	8.34439(2)	8.35156(2)	8.35917(3)
V (Å)^3	744.427(1)	752.006(2)	761.184(5)	3091.19(1)	717.724(3)	720.132(3)	722.057(4)

λ = 0.41283(2) Å for samples 1, 6, and 16; λ = 0.41284(2) Å for the remaining samples. 2θ range used in the Rietveld refinement is 2 to 40°. Nepheline and tetrakalsilite structures were refined in space group $P6_3$ (# 173), and kalsilite in space groups $P6_3$ and $P31c$ (# 159). †Ks values are from the original papers (see text). ‡Ks values are from Rietveld refinements in this study. Two phases: 12a = 79.6(2) and 12b = 20.4(5) wt. %. *# Var. = total number of variables of which 15 are from background, profile, scale, and 0-shift, whereas about 40 are structural variables for nepheline and 122 for tetrakalsilite). Note that N_{obs} / # Var. ≈ 25 for nepheline and ≈ 38 for tetrakalsilite.

TABLE 2b. Unit-cell and Rietveld-refinement parameters for six kalsilite samples that contain mixtures of $P6_3$ (top) and $P31c$ (bottom) phases

$P6_3$	3a	4a	5a	**14a**	**15a**	19a
	8807	8719	8860	8828	8823	9507
Ks†	0.736	0.937	0.948	0.79	0.983	0.875
Ks(ref)‡	0.799(5)	1	1	0.914(1)	1	0.814(4)
χ^2	5.715	2.793	5.298	4.727	1.773	3.793
R_F^2	0.0867	0.0579	0.0644	0.0899	0.0544	0.0814
N_{obs}	717	691	686	927	680	708
a (Å)	5.13933(2)	5.16055(2)	5.16105(3)	5.13825(1)	5.16205(1)	5.1711(1)
c (Å)	8.60735(5)	8.70195(5)	8.70676(7)	8.61016(2)	8.71126(2)	8.6114(3)
V (Å)^3	196.885(2)	200.696(1)	200.846(2)	196.866(1)	201.028(1)	199.423(9)
Wt. %	83.76(4)	30.2(1)	22.2(2)	99.32(1)	55.4(1)	22.1(1)
$P31c$	3b	4b	5b	**14b**	**15b**	19b
Ks(ref)	0.912(22)	0.938(1)	0.953(2)	1	0.971(2)	0.927(2)
a (Å)	5.14585(11)	5.15938(1)	5.15976(1)	5.1452(2)	5.16112(1)	5.16110(2)
c (Å)	8.63409(31)	8.69430(2)	8.69899(2)	8.6249(8)	8.71709(1)	8.66062(7)
V (Å)^3	197.999(9)	200.429(1)	200.567(1)	197.74(2)	201.090(1)	199.786(2)
Wt. %	16.2(2)	69.8(1)	77.8(1)	0.68(4)	44.6(1)	77.9(1)

Phase 14b is 0.68(4) wt. %, so the results are not too reliable. λ = 0.41284(2) Å and # Var. = 31 for all kalsilite samples. N_{obs} / # Var. ≈ 20 for kalsilite.

This is the peer-reviewed, final accepted version for American Mineralogist, published by the Mineralogical Society of America.
The published version is subject to change. Cite as Authors (Year) Title. American Mineralogist, in press.
DOI: https://doi.org/10.2138/am-2021-7484. http://www.minsocam.org/

TABLE 3a. Atom coordinates, isotropic displacement parameters (U x 100 Å^2), and *sofs* for 11 nepheline samples

			1	**6**	**7**	**8**	**9**	**10**
Atom	site		8311	880408	8824	8825	8826	8827
Ks			0.129	0.05	0.108	0.162	0.218	0.315
Ks(ref)			0.156	0.120	0.112	0.203	0.228	0.349
Si1	2*b*	*x*	⅔	⅔	⅔	⅔	⅔	⅔
		y	⅓	⅓	⅓	⅓	⅓	⅓
		z	0.1953(3)	0.1944(4)	0.1949(2)	0.1942(3)	0.1945(3)	0.1932(3)
		U	1.031(8)	1.008(9)	1.082(5)	1.079(5)	1.015(5)	0.956(5)
Al1	2*b*	*x*	⅔	⅔	⅔	⅔	⅔	⅔
		y	⅓	⅓	⅓	⅓	⅓	⅓
		z	0.8088(4)	0.8043(4)	0.8062(2)	0.8065(3)	0.8059(3)	0.8049(3)
		U	1.031(8)	1.008(9)	1.082(5)	1.079(5)	1.015(5)	0.956(5)
Al2	6*c*	*x*	0.3353(2)	0.3326(3)	0.3332(2)	0.3328(2)	0.3335(2)	0.3340(2)
		y	0.0931(2)	0.0920(3)	0.0929(2)	0.0930(2)	0.0932(2)	0.0952(2)
		z	0.3123(1)	0.3130(1)	0.3124(1)	0.3124(1)	0.3124(1)	0.3125(1)
		U	1.031(8)	1.008(9)	1.082(5)	1.079(5)	1.015(5)	0.956(5)
Si2	6*c*	*x*	0.3303(2)	0.3302(3)	0.3314(2)	0.3329(2)	0.3330(2)	0.3323(2)
		y	0.0939(2)	0.0928(3)	0.0931(2)	0.0935(2)	0.0933(2)	0.0943(2)
		z	0.6871(1)	0.6860(1)	0.6862(1)	0.6859(1)	0.6861(1)	0.6865(1)
		U	1.031(8)	1.008(9)	1.082(5)	1.079(5)	1.015(5)	0.956(5)
K	2*a*	*x*	0	0	0	0	0	0
		y	0	0	0	0	0	0
		z	0.9920(6)	0.9964(21)	1.0013(10)	0.9948(4)	0.9949(3)	0.9946(3)
		U	2.83(5)	4.02(22)	1.93(26)	3.07(3)	2.40(2)	2.19(2)
		sof	0.623(2)	0.48(3)	0.45(4)	0.813(2)	0.912(1)	0.957(1)
Na(K)	6*c*	*x*	---	-0.0202(23)	-0.0035(22)	---	---	---
		y	---	0.0444(31)	0.0335(28)	---	---	---
		z	---	1.0003(73)	0.9828(23)	---	---	---
		U	---	1.9(7)	5.9(4)	---	---	---
		sof	---	0.09(1)	0.17(2)	---	---	---
Na1	6*c*	*x*	0.4431(1)	0.4454(1)	0.4450(1)	0.4443(1)	0.4444(1)	0.4445(1)
		y	0.9974(1)	1.0001(1)	0.9995(1)	0.9988(1)	0.9988(1)	0.9973(1)
		z	0.9941(4)	0.9952(5)	0.9964(3)	0.9965(4)	0.9960(3)	0.9967(3)
		U	2.21(3)	2.34(2)	2.46(1)	2.41(2)	2.41(2)	2.04(2)
Na		*sof*	0.972(2)	1	1	1	1	0.81(2)
Ca		*sof*	0.028(2)	---	---	---	---	---

K		*sof*	---	---	---	---	---	0.15(1)
O1	6*c*	*x*	0.7107(6)	0.7076(5)	0.7105(3)	0.7075(4)	0.7069(3)	0.7040(3)
		y	0.3355(11)	0.3414(8)	0.3429(7)	0.3402(8)	0.3420(8)	0.3444(7)
		z	0.9839(10)	1.0059(4)	1.0047(3)	1.0051(4)	1.0041(4)	1.0044(3)
		U	2.04(2)	1.91(2)	2.04(1)	2.04(1)	1.90(1)	1.71(1)
		sof	⅓	⅓	⅓	⅓	⅓	⅓
O2	6*c*	*x*	0.3187(1)	0.3100(2)	0.3120(1)	0.3135(1)	0.3146(1)	0.3149(1)
		y	0.0291(1)	0.0219(2)	0.0235(1)	0.0247(1)	0.0259(1)	0.0287(1)
		z	0.4942(6)	0.4993(7)	0.5000(4)	0.4992(5)	0.4992(5)	0.4990(4)
		U	2.04(2)	1.91(2)	2.04(1)	2.04(1)	1.90(1)	1.71(1)
O3	6*c*	*x*	0.5198(3)	0.5193(3)	0.5197(2)	0.5201(2)	0.5207(2)	0.5205(2)
		y	0.1708(3)	0.1702(3)	0.1708(2)	0.1708(2)	0.1694(2)	0.1717(2)
		z	0.7189(3)	0.7176(3)	0.7182(2)	0.7204(2)	0.7209(2)	0.7224(2)
		U	2.04(2)	1.91(2)	2.04(1)	2.04(1)	1.90(1)	1.71(1)
O4	6*c*	*x*	0.5136(3)	0.5127(3)	0.5122(2)	0.5131(3)	0.5135(2)	0.5125(2)
		y	0.1649(3)	0.1643(3)	0.1649(2)	0.1646(3)	0.1653(2)	0.1665(2)
		z	0.2339(3)	0.2400(3)	0.2393(2)	0.2397(2)	0.2390(2)	0.2412(2)
		U	2.04(2)	1.91(2)	2.04(1)	2.04(1)	1.90(1)	1.71(1)
O5	6*c*	*x*	0.2840(3)	0.2793(4)	0.2814(2)	0.2821(3)	0.2825(2)	0.2839(2)
		y	0.2321(4)	0.2291(5)	0.2292(3)	0.2297(4)	0.2284(3)	0.2296(3)
		z	0.3115(5)	0.3113(6)	0.3113(4)	0.3116(5)	0.3115(4)	0.3114(4)
		U	2.04(2)	1.91(2)	2.04(1)	2.04(1)	1.90(1)	1.71(1)
O6	6*c*	*x*	0.2690(3)	0.2643(4)	0.2640(2)	0.2646(3)	0.2651(2)	0.2626(2)
		y	0.2208(4)	0.2176(5)	0.2186(3)	0.2187(4)	0.2188(3)	0.2186(3)
		z	0.6885(5)	0.6821(6)	0.6840(4)	0.6851(5)	0.6863(4)	0.6898(4)
		U	2.04(2)	1.91(2)	2.04(1)	2.04(1)	1.90(1)	1.71(1)

The *sof* for O1 is fixed at ⅓. Other sites are fully occupied. K, Ca, and Na atoms were used to determine the *sofs* for the K, Na(K), and Na1 sites. *U* for the *T* sites as well as *U* for the O sites are constrained to be the same in each sample.

This is the peer-reviewed, final accepted version for American Mineralogist, published by the Mineralogical Society of America.
The published version is subject to change. Cite as Authors (Year) Title. American Mineralogist, in press.
DOI: https://doi.org/10.2138/am-2021-7484. http://www.minsocam.org/

TABLE 3a. Contd.

Atom	site		**11**	**12a**	**12b**	16	17	18
Ks			8834	8853	8853	9504	9514	9508
			0.409	0.499	?	0	0.052	0.101
Ks(ref)			0.390	0.466	0.567	0.000	0.070	0.118
Si1	2*b*	*x*	⅔	⅔	⅔	⅔	⅔	⅔
		y	⅓	⅓	⅓	⅓	⅓	⅓
		z	0.1915(5)	0.1913(7)	0.1846(16)	0.1941(4)	0.1944(5)	0.1953(4)
		U	1.002(6)	1.302(9)	1.302(9)	0.971(10)	0.962(9)	0.957(9)
Al1	2*b*	*x*	⅔	⅔	⅔	⅔	⅔	⅔
		y	⅓	⅓	⅓	⅓	⅓	⅓
		z	0.8028(5)	0.8024(7)	0.7978(16)	0.8065(5)	0.8078(5)	0.8091(4)
		U	1.002(6)	1.302(9)	1.302(9)	0.971(10)	0.962(9)	0.957(9)
Al2	6*c*	*x*	0.3346(2)	0.3325(4)	0.3374(7)	0.3340(3)	0.3334(3)	0.3340(3)
		y	0.0985(2)	0.1003(4)	0.1065(8)	0.0956(3)	0.0955(3)	0.0954(3)
		z	0.3128(1)	0.3125(4)	0.3133(4)	0.3121(1)	0.3111(5)	0.3124(3)
		U	1.002(6)	1.302(9)	1.302(9)	0.971(10)	0.962(9)	0.957(9)
Si2	6*c*	*x*	0.3316(2)	0.3318(4)	0.3258(7)	0.3297(3)	0.3313(3)	0.3321(3)
		y	0.0960(2)	0.0977(3)	0.0957(7)	0.0927(3)	0.0935(3)	0.0939(3)
		z	0.6863(1)	0.6863(1)	0.6855(1)	0.6855(1)	0.6851(5)	0.6864(1)
		U	1.002(6)	1.302(9)	1.302(9)	0.971(10)	0.962(9)	0.957(9)
K	2*a*	*x*	0	0	0	---	0	0
		y	0	0	0	---	0	0
		z	0.9938(4)	0.9961(7)	0.9992(16)	---	1.0088(28)	1.0019(9)
		U	2.13(3)	2.64(4)	1.34(14)	---	1.9(7)	2.94(9)
		sof	0.959(2)	0.960(2)	0.930(6)	---	0.28(4)	0.472(2)
Na(K)	6*c*	*x*	---	---	---	0.0012(19)	0.0099(40)	---
		y	---	---	---	0.0434(12)	0.0583(92)	---
		z	---	---	---	1.014(1)	0.9970(67)	---
		U	---	---	---	2.6(4)	3.3(11)	---
		sof	---	---	---	0.178(1)	0.07(2)	---
Na1	6*c*	*x*	0.4450(1)	0.4448(1)	0.4450(3)	0.4439(1)	0.4434(1)	0.4433(1)
		y	0.9959(1)	0.9955(1)	0.9946(3)	0.9988(1)	0.9979(1)	0.9975(1)
		z	0.9968(4)	0.9986(6)	0.9891(11)	0.9905(5)	0.9909(7)	0.9924(5)
		U	2.00(2)	2.34(3)	1.95(10)	2.50(3)	2.56(3)	2.53(3)
Na1		*sof*	0.800(2)	0.699(3)	0.554(9)	1	1	1
Ca1		*sof*	----	---	---	---	---	---
K1		*sof*	0.200(2)	0.301(3)	0.446(9)	---	---	---

O1	6*c*	*x*	0.6992(5)	0.6968(6)	0.6883(25)	0.7095(6)	0.7121(6)	0.7121(6)
		y	0.3411(11)	0.3503(16)	0.3284(32)	0.3361(9)	0.3376(11)	0.3387(11)
		z	1.0027(5)	1.0023(7)	0.9985(16)	1.0069(5)	1.0069(6)	1.0077(5)
		U	1.81(2)	2.07(2)	2.07(2)	2.22(3)	2.16(2)	2.06(2)
		sof	⅓	⅓	⅓	⅓	⅓	⅓
O2	6*c*	*x*	0.3152(1)	0.3147(2)	0.3110(6)	0.3155(2)	0.3171(2)	0.3184(2)
		y	0.0331(1)	0.0362(2)	0.0397(5)	0.0287(2)	0.0303(2)	0.0313(2)
		z	0.4997(6)	0.5030(8)	0.5001(21)	0.4970(8)	0.4967(8)	0.4980(8)
		U	1.81(2)	2.07(2)	2.07(2)	2.22(3)	2.16(2)	2.06(2)
O3	6*c*	*x*	0.5205(3)	0.5159(4)	0.5164(12)	0.5182(4)	0.5182(3)	0.5197(3)
		y	0.1748(3)	0.1778(4)	0.1846(10)	0.1691(4)	0.1711(4)	0.1700(4)
		z	0.7246(3)	0.7258(4)	0.7296(16)	0.7153(4)	0.7151(6)	0.7165(4)
		U	1.81(2)	2.07(2)	2.07(2)	2.22(3)	2.16(2)	2.06(2)
O4	6*c*	*x*	0.5093(3)	0.5119(5)	0.5113(12)	0.5133(4)	0.5141(3)	0.5130(3)
		y	0.1683(3)	0.1680(4)	0.1599(10)	0.1695(4)	0.1680(4)	0.1686(4)
		z	0.2429(3)	0.2410(4)	0.2429(18)	0.2359(4)	0.2342(6)	0.2344(4)
		U	1.81(2)	2.07(2)	2.07(2)	2.22(3)	2.16(2)	2.06(2)
O5	6*c*	*x*	0.2823(3)	0.2817(4)	0.2534(13)	0.2726(7)	0.2748(7)	0.2759(7)
		y	0.2297(4)	0.2320(5)	0.2209(14)	0.2286(8)	0.2293(7)	0.2298(7)
		z	0.3085(5)	0.3066(7)	0.2939(13)	0.3061(7)	0.3049(6)	0.3061(7)
		U	1.81(2)	2.07(2)	2.07(2)	2.22(3)	2.16(2)	2.06(2)
O6	6*c*	*x*	0.2610(3)	0.2609(4)	0.2791(13)	0.2775(7)	0.2771(6)	0.2770(6)
		y	0.2202(4)	0.2185(5)	0.2275(13)	0.2259(7)	0.2258(7)	0.2256(7)
		z	0.6908(5)	0.6923(7)	0.6808(14)	0.6816(7)	0.6820(6)	0.6844(7)
		U	1.81(2)	2.07(2)	2.07(2)	2.22(3)	2.16(2)	2.06(2)

This is the peer-reviewed, final accepted version for American Mineralogist, published by the Mineralogical Society of America.
The published version is subject to change. Cite as Authors (Year) Title. American Mineralogist, in press.
DOI: https://doi.org/10.2138/am-2021-7484. http://www.minsocam.org/

TABLE 3b. Atom coordinates, isotropic displacement parameters (U x 100 Å^2), and *sofs* for one tetrakalsilite (sample 13 = 8843; Ks = 0.698)

Atom	site	*x*	*y*	*z*	*U*	*sof*	Atom	site	*x*	*y*	*z*	*U*
Si1	6*c*	0.0386(3)	0.1595(3)	0.5885(11)	0.92(2)	1	O1	6*c*	0.1439(4)	0.1374(4)	0.2653(12)	1.31(4)
Si2	6*c*	0.3318(3)	0.1933(3)	0.5825(11)	0.92(2)	1	O2	6*c*	0.1167(4)	0.3143(4)	0.2661(13)	1.31(4)
Si3	6*c*	0.3062(3)	0.4050(3)	0.5810(11)	0.92(2)	1	O3	6*c*	0.3990(4)	0.1198(4)	0.2621(12)	1.31(4)
Si4	6*c*	0.5965(3)	0.4325(3)	0.5723(5)	0.92(2)	1	O4	6*c*	0.1541(4)	0.5792(4)	0.2593(6)	1.31(4)
Si5	6*c*	0.0680(3)	0.4194(3)	0.5814(11)	0.92(2)	1	O5	6*c*	0.3983(4)	0.3477(4)	0.2645(12)	1.31(4)
Si6	2*b*	⅓	⅔	0.5710(13)	0.92(2)	1	O6	2*b*	⅔	⅓	0.2612(14)	1.31(4)
							O7	6*c*	0.1372(6)	0.4068(5)	0.5229(20)	1.31(4)
							O8	6*c*	0.1029(5)	0.1358(7)	0.5906(15)	1.31(4)
Al1	6*c*	0.1604(4)	0.1234(3)	0.4567(10)	0.92(2)	1	O9	6*c*	0.3420(6)	0.1198(5)	0.5689(17)	1.31(4)
Al2	6*c*	0.1414(3)	0.3279(3)	0.4636(12)	0.92(2)	1	O10	6*c*	0.4060(5)	0.2706(4)	0.5271(19)	1.31(4)
Al3	6*c*	0.4043(3)	0.1036(3)	0.4594(11)	0.92(2)	1	O11	6*c*	-0.0184(4)	0.3729(6)	0.5063(14)	1.31(4)
Al4	6*c*	0.1628(3)	0.5863(3)	0.4622(10)	0.92(2)	1	O12	6*c*	0.4894(4)	0.1765(4)	0.5438(13)	1.31(4)
Al5	6*c*	0.4232(3)	0.3582(3)	0.4600(11)	0.92(2)	1	O13	6*c*	0.1334(6)	0.0285(5)	0.4662(15)	1.31(4)
Al6	2*b*	⅔	⅓	0.4639(13)	0.92(2)	1	O14	6*c*	0.3510(4)	0.4950(4)	0.5443(12)	1.31(4)
							O15	6*c*	0.3701(5)	0.3812(6)	0.5844(14)	1.31(4)
							O16	6*c*	0.2488(3)	0.5982(3)	0.5281(14)	1.31(4)
Na	6*c*	-0.0206(3)	0.2587(3)	0.7811(14)	1.85(3)	1.07(1)	O17	6*c*	0.0925(6)	0.5066(4)	0.5502(16)	1.31(4)
K1	6*c*	0.5026(2)	0.2665(2)	0.2651(12)	1.85(3)	0.82(2)	O18	6*c*	0.2559(5)	0.1838(6)	0.4974(18)	1.31(4)
K2	6*c*	-0.0039(2)	0.4757(2)	0.2748(14)	1.85(3)	0.66(1)	O19	6*c*	0.5182(4)	0.4170(6)	0.4915(15)	1.31(4)
K3	6*c*	0.2401(2)	0.4983(2)	0.2790(10)	1.85(3)	1.03(1)	O20	6*c*	0.6025(3)	0.3565(3)	0.5432(14)	1.31(4)
K4	6*c*	0.2421(2)	0.0308(2)	0.2782(12)	1.85(3)	0.74(1)	O21	6*c*	0.0730(6)	0.2489(4)	0.5625(17)	1.31(4)
K5	2*a*	0	0	0.7747(22)	1.85(3)	0.89(1)	O22	6*c*	0.2320(4)	0.3405(6)	0.4860(17)	1.31(4)

The *sof* for all the O atoms is 1. The K1 site also contains 0.18(2) Na, K2 site contains 0.34(1) Na, and K4 site contains 0.26(1) Na. The chemical formula from the refinement is $(K_{0.666}Na_{0.346})[AlSiO_4]$, so Ks = 0.666.

This is the peer-reviewed, final accepted version for American Mineralogist, published by the Mineralogical Society of America.
The published version is subject to change. Cite as Authors (Year) Title. American Mineralogist, in press.
DOI: https://doi.org/10.2138/am-2021-7484. http://www.minsocam.org/

TABLE 3c. Atom coordinates, isotropic displacement parameters (U x 100 Å^2), and *sofs* for six $P6_3$ kalsilite samples

			3a	4a	5a	**14a**	**15a**	19a
	site		8807	8719	8860	8828	8823	9507
Wt. %			83.76(4)	30.2(1)	22.2(2)	99.32(1)	55.4(1)	22.1(1)
Ks			0.736	0.937	0.948	0.79	0.983	0.875
Ks(ref)			0.799(5)	1	1	0.914(1)	1	0.814(4)
Al1	2*b*	*x*	⅓	⅓	⅓	⅓	⅓	⅓
		y	⅔	⅔	⅔	⅔	⅔	⅔
		z	0.0587(6)	0.0613(6)	0.4419(15)	0.0581(3)	0.0596(3)	0.4497(14)
		U	1.31(2)	0.88(3)	0.76(1)	1.27(1)	0.95(2)	1.18(1)
Si1	2*b*	*x*	⅓	⅓	⅓	⅓	⅓	⅓
		y	⅔	⅔	⅔	⅔	⅔	⅔
		z	0.4399(6)	0.4432(5)	0.0603(15)	0.4393(3)	0.4419(3)	0.0673(14)
		U	1.31(2)	0.88(3)	0.76(1)	1.27(1)	0.95(2)	1.18(1)
(K,Na)1	2*a*	*x*	0	0	0	0	0	0
		y	0	0	0	0	0	0
		z	¼	¼	¼	¼	¼	¼
		U	2.21(3)	1.45(4)	1.78(1)	2.16(2)	1.72(2)	2.29(2)
K1		*sof*	0.799(5)	1	1	0.914(1)	1	0.814(4)
Na1		*sof*	0.149(5)	0	0	0	0	0
O1	6*c*	*x*	0.3355(17)	0.3445(56)	0.3475(69)	0.4065(6)	0.3508(33)	0.3654(47)
		y	0.7435(10)	0.6934(32)	0.6956(38)	0.7440(5)	0.7006(13)	0.6200(44)
		z	0.2542(8)	0.2587(6)	0.2442(15)	0.2544(4)	0.2572(3)	0.2513(14)
		U	1.95(4)	2.15(7)	1.70(3)	2.09(2)	1.76(3)	1.31(3)
		sof	⅓	⅓	⅓	⅓	⅓	⅓
O2	6*c*	*x*	0.3907(4)	0.4069(4)	0.4267(5)	0.3934(2)	0.3964(2)	0.4580(7)
		y	-0.0003(8)	0.0025(4)	0.0197(6)	-0.0003(4)	0.0013(3)	0.0213(10)
		z	0.4809(5)	0.4819(5)	0.4890(15)	0.4814(3)	0.4850(3)	0.5119(14)
		U	1.95(4)	2.15(7)	1.70(3)	2.09(2)	1.76(3)	1.31(3)

The *sof* = 1 for Al1, Si1, and O2. K1 and Na1 are at the same site and the sum of their *sofs* were constrained to the chemical composition where possible (Table 1). Also, U (Al1) = U (Si1), and U (O1) = U (O2).

This is the peer-reviewed, final accepted version for American Mineralogist, published by the Mineralogical Society of America.
The published version is subject to change. Cite as Authors (Year) Title. American Mineralogist, in press.
DOI: https://doi.org/10.2138/am-2021-7484. http://www.minsocam.org/

TABLE 3d. Atom coordinates, isotropic displacement parameters (U x 100 Å^2), and *sofs* for six *P*31*c* kalsilite samples

			3b	4b	5b	**14b**	**15b**	19b
	site		8807	8719	8860	8828	8823	9507
Wt. %			16.2(2)	69.8(1)	77.8(1)	0.68(4)	44.6(1)	77.9(1)
Ks			0.736	0.937	0.948	0.79	0.983	0.875
Ks(ref)			0.912(22)	0.938(1)	0.953(2)	1	0.971(2)	0.927(2)
Al1	2*b*	*x*	⅓	⅓	⅓		⅓	⅓
		y	⅔	⅔	⅔		⅔	⅔
		z	0.0553(18)	0.4417(9)	0.0605(6)		0.0587(6)	0.0594(10)
		U	0.48(7)	0.75(1)	0.76(1)		0.61(2)	1.18(1)
Si1	2*b*	*x*	⅓	⅓	⅓		⅓	⅓
		y	⅔	⅔	⅔		⅔	⅔
		z	0.4399(19)	0.0604(9)	0.4418(5)		0.4396(6)	0.4396(10)
		U	0.48(7)	0.75(1)	0.76(1)		0.61(2)	1.18(1)
(K,Na)1	2*a*	*x*	0	0	0		0	0
		y	0	0	0		0	0
		z	¼	¼	¼		¼	¼
		U	2.08(14)	1.95(2)	1.78(1)		1.58(2)	2.29(2)
K1		*sof*	0.912(22)	0.938(1)	0.953(2)	1	0.971(2)	0.927(2)
Na1		*sof*	0.036(22)	0	0		0	0
O1	6*c*	*x*	0.2637(35)	0.2777(9)	0.2872(12)		0.2849(11)	0.2703(8)
		y	0.6084(47)	0.6611(14)	0.6628(24)		0.6185(10)	0.6321(37)
		z	0.2540(19)	0.2441(9)	0.2573(6)		0.2560(6)	0.2545(11)
		U	2.57(21)	0.78(8)	1.70(3)		1.01(3)	1.31(3)
		sof	⅓	⅓	⅓		⅓	⅓
O2	6*c*	*x*	0.5809(12)	0.6004(3)	0.6114(3)		0.6205(3)	0.6077(5)
		y	-0.0075(12)	-0.0145(4)	0.0048(5)		0.0176(3)	0.0027(9)
		z	-0.0291(15)	-0.0019(9)	-0.0086(6)		0.0052(7)	-0.0091(8)
		U	2.57(21)	0.78(8)	1.70(3)		1.01(3)	1.31(3)

This is the peer-reviewed, final accepted version for American Mineralogist, published by the Mineralogical Society of America.
The published version is subject to change. Cite as Authors (Year) Title. American Mineralogist, in press.
DOI: https://doi.org/10.2138/am-2021-7484. http://www.minsocam.org/

TABLE 4a. Bond distances [Å] and angles [°] for 11 nepheline samples

	1	**6**	**7**	**8**	**9**	**10**
	8311	880408	8824	8825	8826	8827
Si1-O1 x 1	1.633(2)	1.619(2)	1.640(2)	1.628(2)	1.638(2)	1.623(2)
Si1-O4 x 3	1.653(2)	1.660(3)	1.658(2)	1.660(2)	1.654(2)	1.665(2)
<Si1-O>[4]	**1.648**	**1.649**	**1.654**	**1.652**	**1.650**	**1.655**
Al1-O1 x 1	1.715(2)	1.725(2)	1.708(2)	1.706(2)	1.702(2)	1.711(2)
Al1-O3 x 3	1.720(3)	1.715(3)	1.717(2)	1.710(2)	1.713(2)	1.699(2)
<Al1-O>[4]	**1.719**	**1.717**	**1.714**	**1.709**	**1.710**	**1.702**
Al2-O2	1.639(5)	1.675(5)	1.686(3)	1.679(4)	1.678(4)	1.678(4)
Al2-O4	1.678(3)	1.680(4)	1.673(2)	1.685(3)	1.687(2)	1.675(2)
Al2-O5	1.703(4)	1.695(5)	1.680(3)	1.678(4)	1.667(3)	1.659(3)
Al2-O6	1.671(4)	1.685(5)	1.670(3)	1.667(4)	1.667(3)	1.656(3)
<Al2-O>[4]	**1.673**	**1.684**	**1.677**	**1.677**	**1.675**	**1.667**
Si2-O2	1.714(4)	1.683(5)	1.677(3)	1.679(4)	1.679(4)	1.684(3)
Si2-O3	1.671(3)	1.663(3)	1.658(2)	1.654(3)	1.661(2)	1.673(2)
Si2-O5	1.650(4)	1.645(5)	1.661(3)	1.672(4)	1.682(3)	1.690(3)
Si2-O6	1.660(4)	1.672(5)	1.692(3)	1.698(4)	1.700(3)	1.710(3)
<Si2-O>[4]	**1.674**	**1.666**	**1.672**	**1.676**	**1.681**	**1.689**
K-O2 x 3	3.053(1)	2.987(1)	3.003(1)	3.017(1)	3.025(1)	3.029(1)
K-O5 x 3	3.035(4)	3.000(9)	3.037(5)	3.016(3)	3.019(3)	3.040(3)
K-O6 x 3	2.965(4)	2.887(10)	2.879(5)	2.920(3)	2.931(3)	2.947(3)
<K-O>[9]	**3.018**	**2.958**	**2.973**	**2.984**	**2.992**	**3.005**
Na(K)-O2	---	2.884(16)	2.853(20)	---	---	---
Na(K)-O2	---	2.622(26)	2.841(21)	---	---	---
Na(K)-O5	---	2.61(5)	2.667(30)	---	---	---
Na(K)-O5	---	3.091(32)	3.058(17)	---	---	---
Na(K)-O6	---	2.47(4)	2.691(14)	---	---	---
Na(K)-O6	---	2.95(4)	3.063(23)	---	---	---
Na(K)-O6	---	---	---	---	---	---
<Na(K)-O>	---	**2.771**	**2.862**	---	---	---
Na1-O1	2.557(4)	2.560(4)	2.544(2)	2.576(3)	2.587(3)	2.640(2)
Na1-O2	2.519(1)	2.555(2)	2.548(1)	2.545(1)	2.544(1)	2.557(1)
Na1-O3	2.750(3)	2.747(4)	2.761(3)	2.752(3)	2.740(3)	2.763(3)
Na1-O3	2.677(3)	2.656(4)	2.655(3)	2.668(3)	2.664(3)	2.685(2)
Na1-O4	2.490(3)	2.493(4)	2.489(3)	2.495(3)	2.501(3)	2.534(3)
Na1-O4	2.859(3)	2.844(4)	2.864(2)	2.858(3)	2.865(3)	2.867(2)
Na1-O5	2.447(4)	2.486(5)	2.488(3)	2.483(3)	2.489(3)	2.498(3)
Na1-O6	2.603(4)	2.599(4)	2.599(3)	2.601(3)	2.612(3)	2.649(2)
<Na1-O>[8]	**2.613**	**2.618**	**2.619**	**2.622**	**2.625**	**2.649**
<Na1-O>[7]	**2.621**	**2.626**	**2.629**	**2.629**	**2.631**	**2.650**
O1-O1	0.743(5)	0.649(6)	0.690(4)	0.656(4)	0.635(4)	0.577(4)
Si1-O1-Al1	150.3(2)	154.1(2)	152.5(1)	153.7(2)	154.6(2)	156.9(1)
Al2-O2-Si2	138.8(1)	136.3(1)	136.9(1)	137.3(1)	138.0(1)	138.7(1)
Al1-O3-Si2	137.9(2)	137.9(2)	138.1(1)	138.5(2)	137.6(1)	138.9(1)
Si1-O4-Al2	139.1(2)	140.0(2)	140.3(2)	139.8(2)	140.0(2)	140.8(2)
Al2-O5-Si2	141.6(3)	140.9(3)	141.2(2)	141.2(2)	141.6(2)	141.8(2)
Al2-O6-Si2	140.3(3)	137.3(3)	138.2(2)	138.8(2)	139.5(2)	140.9(2)
<T-O-T>[6]	**141.34**	**141.09**	**141.18**	**141.55**	**141.87**	**142.99**

Based on average <T-O> distances, high Al-Si disorder occurs in all nepheline samples.

This is the peer-reviewed, final accepted version for American Mineralogist, published by the Mineralogical Society of America.
The published version is subject to change. Cite as Authors (Year) Title. American Mineralogist, in press.
DOI: https://doi.org/10.2138/am-2021-7484. http://www.minsocam.org/

TABLE 4a. Contd.

	11	**12a**	**12b**	16	17	18
	8834	8853	8853	9504	9514	9508
Si1-O1 x 1	1.621(2)	1.620(3)	1.598(5)	1.616(2)	1.626(3)	1.627(3)
Si1-O4 x 3	1.685(2)	1.678(4)	1.752(10)	1.621(3)	1.624(3)	1.626(3)
<Si1-O>[4]	**1.669**	**1.663**	**1.714**	**1.620**	**1.625**	**1.626**
Al1-O1 x 1	1.713(2)	1.712(3)	1.721(5)	1.723(2)	1.718(3)	1.715(3)
Al1-O3 x 3	1.677(3)	1.682(4)	1.629(11)	1.739(4)	1.737(3)	1.738(3)
<Al1-O>[4]	**1.686**	**1.689**	**1.652**	**1.735**	**1.732**	**1.732**
Al2-O2	1.682(5)	1.712(6)	1.692(18)	1.654(6)	1.657(6)	1.656(6)
Al2-O4	1.647(3)	1.701(6)	1.679(13)	1.680(4)	1.697(4)	1.688(4)
Al2-O5	1.654(4)	1.654(6)	1.763(14)	1.717(6)	1.705(6)	1.709(6)
Al2-O6	1.657(4)	1.670(6)	1.818(11)	1.708(7)	1.699(6)	1.696(7)
<Al2-O>[4]	**1.660**	**1.684**	**1.738**	**1.690**	**1.690**	**1.687**
Si2-O2	1.675(5)	1.647(6)	1.654(18)	1.677(6)	1.675(6)	1.675(6)
Si2-O3	1.690(3)	1.654(5)	1.723(13)	1.656(4)	1.642(4)	1.651(4)
Si2-O5	1.681(4)	1.667(5)	1.515(10)	1.585(6)	1.597(6)	1.603(6)
Si2-O6	1.725(4)	1.703(6)	1.632(13)	1.650(6)	1.658(5)	1.661(5)
<Si2-O>[4]	**1.693**	**1.668**	**1.631**	**1.642**	**1.643**	**1.648**
K-O2 x 3	3.028(1)	3.022(2)	2.985(6)	---	3.026(2)	3.036(2)
K-O5 x 3	3.055(3)	3.087(5)	2.991(15)	---	3.063(13)	3.035(6)
K-O6 x 3	2.965(3)	2.965(5)	3.038(14)	---	2.930(12)	2.970(6)
<K-O>[9]	**3.016**	**3.025**	**3.005**	---	**3.006**	**3.014**
Na(K)-O2	---	---	---	2.786(15)	2.68(6)	---
Na(K)-O2	---	---	---	2.869(16)	2.922(31)	---
Na(K)-O5	---	---	---	2.727(9)	2.57(7)	---
Na(K)-O5	---	---	---	---	---	---
Na(K)-O6	---	---	---	2.545(10)	2.53(8)	---
Na(K)-O6	---	---	---	3.069(15)	---	---
Na(K)-O6	---	---	---	3.160(12)	---	---
<Na(K)-O>[4, 6]	---	---	---	**2.799**	**2.676**	---
Na1-O1	2.703(3)	2.757(7)	2.822(20)	2.548(4)	2.536(4)	2.544(4)
Na1-O2	2.579(1)	2.613(2)	2.677(7)	2.546(2)	2.543(2)	2.536(2)
Na1-O3	2.783(3)	2.815(4)	2.777(12)	2.729(5)	2.749(4)	2.749(4)
Na1-O3	2.716(3)	2.763(5)	2.891(13)	2.663(4)	2.673(4)	2.657(4)
Na1-O4	2.575(3)	2.556(5)	2.605(14)	2.528(5)	2.512(4)	2.512(4)
Na1-O4	2.884(3)	2.900(5)	2.781(15)	2.868(4)	2.867(4)	2.884(4)
Na1-O5	2.535(3)	2.551(5)	2.719(12)	2.498(7)	2.498(6)	2.497(6)
Na1-O6	2.669(3)	2.685(5)	2.594(12)	2.534(7)	2.537(6)	2.545(6)
<Na1-O>[8]	**2.681**	**2.705**	**2.733**	**2.614**	**2.614**	**2.615**
<Na1-O>[7]	**2.677**	**2.698**	**2.721**	**2.624**	**2.626**	**2.626**
O1-O1	0.514(5)	0.459(8)	0.432(28)	0.718(6)	0.752(6)	0.744(6)
Si1-O1-Al1	159.5(2)	161.7(3)	163.0(1)	151.2(3)	149.9(2)	150.2(2)
Al2-O2-Si2	139.7(1)	140.5(1)	141.6(3)	138.7(1)	139.3(1)	139.7(1)
Al1-O3-Si2	140.5(2)	144.2(3)	148.5(7)	137.2(3)	138.3(3)	137.0(2)
Si1-O4-Al2	142.5(2)	140.2(3)	134.5(7)	141.6(3)	140.1(3)	140.8(3)
Al2-O5-Si2	143.4(3)	144.0(4)	145.2(8)	142.1(4)	142.9(4)	143.1(4)
Al2-O6-Si2	141.4(3)	142.9(4)	140.3(7)	139.2(4)	139.7(4)	140.3(4)
<T-O-T>[6]	**144.50**	**145.57**	**145.46**	**141.67**	**141.69**	**141.85**

This is the peer-reviewed, final accepted version for American Mineralogist, published by the Mineralogical Society of America.
The published version is subject to change. Cite as Authors (Year) Title. American Mineralogist, in press.
DOI: https://doi.org/10.2138/am-2021-7484. http://www.minsocam.org/

TABLE 4b. Bond distances [Å] and angles [°] for one tetrakalsilite (sample-**13** = 8843)

Al1-O1	1.720(5)	Al2-O2	1.742(5)	Al3-O3	1.730(5)	Al4-O4	1.739(5)	Al5-O5	1.726(5)	Al6-O6	1.730(6)
Al1-O8	1.746(6)	Al2-O7	1.736(5)	Al3-O9	1.740(5)	Al4-O14	1.666(9)	Al5-O10	1.740(5)	Al6-O20	1.740(5)
Al1-O13	1.734(6)	Al2-O21	1.738(5)	Al3-O11	1.675(9)	Al4-O16	1.746(5)	Al5-O15	1.744(5)	Al6-O20	1.740(5)
Al1-O21	1.748(5)	Al2-O22	1.747(5)	Al3-O12	1.782(5)	Al4-O17	1.716(5)	Al5-O19	1.719(5)	Al6-O20	1.740(5)
<Al-O>[4]	**1.737**		**1.741**		**1.732**		**1.717**		**1.732**		**1.738**
Si1-O1	1.612(7)	Si2-O2	1.619(6)	Si3-O3	1.625(6)	Si4-O4	1.625(5)	Si5-O5	1.613(6)	Si6-O6	1.623(6)
Si1-O8	1.615(5)	Si2-O9	1.623(5)	Si3-O14	1.624(5)	Si4-O12	1.757(10)	Si5-O7	1.636(5)	Si6-O16	1.632(5)
Si1-O13	1.639(9)	Si2-O10	1.621(5)	Si3-O15	1.607(5)	Si4-O19	1.622(5)	Si5-O11	1.660(5)	Si6-O16	1.632(5)
Si1-O21	1.612(5)	Si2-O18	1.634(5)	Si3-O22	1.643(5)	Si4-O20	1.639(5)	Si5-O17	1.616(5)	Si6-O16	1.632(5)
<Si-O>[4]	**1.620**		**1.624**		**1.625**		**1.661**		**1.631**		**1.630**
Na-O1	2.673(8)	K1-O3	2.672(8)	K2-O4	2.847(8)	K3-O4	2.961(9)	K4-O2	2.682(8)	K5-O1 × 3	2.880(7)
Na-O5	2.476(8)	K1-O6	2.923(4)	K2-O5	3.168(8)	K3-O7	2.885(14)	K4-O3	2.791(8)	K5-O8 × 3	2.961(16)
Na-O9	2.536(13)	K1-O7	2.871(15)	K2-O11	2.790(13)	K3-O10	2.954(14)	K4-O8	2.717(12)	K5-O13 × 3	2.978(16)
Na-O18	2.667(14)	K1-O10	3.013(15)	K2-O15	2.647(13)	K3-O12	2.559(9)	K4-O9	3.149(16)		
Na-O21	2.751(13)	K1-O12	2.935(11)	K2-O17	2.926(16)	K3-O14	3.230(9)	K4-O13	2.722(10)		
Na-O22	2.368(14)	K1-O14	3.077(11)	K2-O17	2.784(13)	K3-O16	2.891(10)	K4-O18	3.014(15)		
		K1-O16	2.733(11)	K2-O19	3.057(15)	K3-O20	2.890(10)	K4-O21	3.057(14)		
		K1-O20	3.071(10)	K2-O19	2.765(13)						
<Na-O>[6]	**2.579**	**<K1-O>[8]**	**2.912**	**<K2-O>[8]**	**2.873**	**<K3-O>[7]**	**2.910**	**<K4-O>[7]**	**2.876**	**<K5-O>[9]**	**2.940**

Based on average <T-O> distances, high Al-Si order occurs in tetrakalsilite because the average <Al-O> is close to 1.74 Å and the average <Si-O> is close to 1.62 Å. Soft constraints were used for the T-O distances. Grand mean of <K-O> = 2.902 Å (which is the mean of the five (K1 to K5) average <K-O> distances.

TABLE 4c. Bond distances [Å] and angles [°] for six kalsilite samples

*P*6$_3$	3a	4a	5a	**14a**	**15a**	19a**
	8807	8719	8860	8828	8823	9507
Wt. %	83.76(4)	30.2(1)	22.2(2)	99.32(1)	55.4(1)	22.1(1)
Al-O1 x 1	1.741(2)	1.722(2)	1.726(3)	1.734(2)	1.728(1)	1.731(3)
Al-O2 x 3	1.725(2)	1.703(2)	1.686(3)	1.714(2)	1.708(2)	1.652(3)
†<Al-O>[4]	**1.729**	**1.708**	**1.696**	**1.719**	**1.713**	**1.671**
Si-O1 x 1	1.631(2)	1.610(2)	1.607(3)	1.638(2)	1.616(1)	1.611(3)
Si-O2 x 3	1.621(2)	1.614(2)	1.592(3)	1.621(2)	1.633(2)	1.565(3)
†<Si-O>[4]	**1.623**	**1.613**	**1.596**	**1.625**	**1.629**	**1.576**
(K,Na)-O1 x 3	2.982(7)	2.933(25)	3.110(17)	2.649(3)	2.910(15)	2.793(10)
(K,Na)-O1 x 3	2.646(5)	2.912(24)	2.919(31)	2.974(4)	3.133(6)	2.857(10)
(K,Na)-O1 x 3	3.314(4)	3.100(14)	2.916(31)	3.316(2)	2.906(15)	3.347(7)
(K,Na)-O2 x 3	2.830(3)	2.908(3)	2.994(9)	2.839(2)	2.892(2)	3.072(7)
(K,Na)-O2 x 3	3.061(3)	3.134(4)	3.130(9)	3.072(2)	3.083(2)	3.261(8)
‡<(K,Na)-O>[9]	**2.957**	**3.008**	**3.035**	**2.963**	**2.986**	**3.111**
O1-O1	0.671(4)	0.208(24)	0.224(30)	0.670(3)	0.263(10)	0.626(13)
Al-O1-Si	153.4(2)	172.0(1)	171.1(12)	153.4(1)	169.6(4)	155.0(5)
Al-O2-Si	139.4(1)	143.7(1)	148.2(2)	140.38(6)	141.23(7)	159.1(2)
<T-O-T>[2]	**146.1**	**155.9**	**156.3**	**146.9**	**155.4**	**157.0**
*P*31*c*	3b	4b	5b	**14b***	**15b**	19b
Wt. %	16.2(2)	69.8(1)	77.8(1)	0.68(4)	44.6(1)	77.9(1)
Al-O1 x 1	1.740(3)	1.740(2)	1.728(2)		1.738(1)	1.729(2)
Al-O2 x 3	1.716(3)	1.722(2)	1.720(2)		1.735(1)	1.720(2)
†<Al-O>[4]	**1.722**	**1.726**	**1.722**		**1.736**	**1.722**
Si-O1 x 1	1.624(3)	1.620(2)	1.622(2)		1.619(1)	1.617(2)
Si-O2 x 3	1.612(2)	1.622(2)	1.630(2)		1.628(1)	1.623(2)
†<Si-O>[4]	**1.615**	**1.622**	**1.628**		**1.626**	**1.622**
(K,Na)-O1 x 3	3.279(11)	3.230(4)	3.187(5)		3.199(5)	2.824(10)
(K,Na)-O1 x 3	2.937(14)	2.760(5)	2.794(7)		2.990(7)	3.259(3)
(K,Na)-O1 x 3	2.730(13)	2.967(6)	2.971(11)		2.768(5)	2.880(11)
(K,Na)-O2 x 3	3.273(8)	2.983(6)	3.022(4)		2.928(4)	3.040(4)
(K,Na)-O2 x 3	2.837(7)	2.959(6)	2.912(4)		2.996(4)	2.901(4)
‡<(K,Na)-O>[9]	**3.031**	**2.976**	**2.973**		**2.970**	**2.976**
O1-O1	0.562(18)	0.474(6)	0.396(6)		0.432(6)	0.485(5)
Al-O1-Si	157.7(7)	161.2(2)	164.3(2)		162.9(3)	160.7(2)

Al-O2-Si	141.3(3)	141.01(6)	140.40(8)	139.51(6)	141.23(8)
<T-O-T>[2]	**151.9**	**151.6**	**152.4**	**151.2**	**151.0**

†High Al-Si order occurs in all the samples. ‡Because of O1 disorder, e.g., sample-14a has average <K-O1>[3] = 2.980, so the average <(Na,K)-O>[9] = 2.963 Å (Fig. 2b). *Sample-14b is a minor phase (0.68(4) wt. %), so the distances are not reliable. **Sample-19 contains broad and asymmetrical reflections. Soft constraints were used for the T-O distances.